Lithogeochemical characterisation of cover sequence on Yorke Peninsula, South Australia, and identification of pathfinder elements for IOCG exploration.

Thesis submitted in accordance with the requirements of the University of Adelaide for an Honours Degree in Geology.

Rebecca Louise Hill

November 2015

THE UNIVERSITY of ADELAIDE

LITHOGEOCHEMICAL CHARACTERISATION OF COVER SEQUENCE ON YORKE PENINSULA, SOUTH AUSTRALIA, AND IDENTIFICATION OF PATHFINDER ELEMENTS FOR IOCG EXPLORATION.

GEOCHEMICAL EXPLORATION OF YP COVER ROCKS

ABSTRACT

Discoveries of major ore deposits have declined as the average depth of cover material overlying mineralisation has increased, resulting in a marked increase in the cost of greenfields exploration. In the past, the cover material has been discarded as it was not thought to be of use in exploration, however recently cover sequence geochemistry has been utilised in the exploration for various commodities, including base metals and gold. The Yorke Peninsula, South Australia, hosts economic and sub-economic IOCG deposits within the basement rocks which are overlain by Cambrian – Quaternary cover. Background geochemistry of whole rock samples were statistically determined, and pathfinders As, Co, S, Sb, Cu, Au, Ce and La were identified as potential vectors towards IOCG mineralisation on the Yorke Peninsula. Using the prospectivity index proposed by Fabris et al (2013), with a modified threshold of 3x average crustal abundance for cover rocks, areas of potential expression of basement mineralisation on the Yorke Peninsula were identified. Evidence of mechanical transport of elements from the basement was identified in diamictite samples, while chemical transport is seen in conglomerate samples. Pathfinder elements As and Sb were hosted in remobilised pyrite, while Co and Ni were hosted within primary pyrite grains. If the depositional and post-depositional environment of the cover material is understood, sulphide chemistry is a potential exploration tool for the Yorke Peninsula.

KEYWORDS

IOCG, Yorke Peninsula, exploration, lithogeochemistry, geochemistry, pyrite, pathfinders

TABLE OF CONTENTS

LIST OF FIGURES AND TABLES

INTRODUCTION

Discoveries of major ore deposits in Australia have been declining in the past 20 years as the average depth of cover material required to explore through has increased from <100m in the 1920s to potentially >600m currently (Schodde 2014). This is a result of the majority of exposed and near-surface deposits having been discovered and has caused a marked increase in the costs associated with greenfields exploration (Giles et al. 2014). While the younger cover sediments overlying potentially mineralised crystalline basement rocks were discarded by explorers in the past, it has been demonstrated that the cover sequence geochemistry can be used as an exploration tool for alteration distal to the mineralised region, due to the preservation of pathfinder elements that can be used to vector towards potential mineralisation (Anand et al. 2001, Anand and Butt 2010). Pathfinders for iron oxide-copper-gold (IOCG) deposits have been well characterised in the basement material (Mark et al. 2006, Groves et al. 2010). However, although cover sequences have been effectively demonstrated as a useful tool to explore for numerous commodities, including gold (Fisher et al. 2013, Lintern 2014, Hill et al. 2014, Prendergast 2007) and base metals (Mumm et al. 2012), less is understood about how pathfinder elements are mobilised and preserved within the cover sequence in comparison to mineralised basement rocks.

The Yorke Peninsula in the southern Gawler Craton in South Australia is known to host economic and sub-economic IOCG mineralisation within the Palaeoproterozoic basement rocks of the Wallaroo Group (Cowley et al. 2003), which are extensively overlain by Cambrian to Quaternary cover. These cover lithologies include Permian diamictites and Cambrian conglomerates (Zang 2003). It is not known whether mechanical or chemical transport mechanisms are predominant in the region, however both have been utilised as an exploration tool in other regions - mechanically transported material has been utilised in glacially derived cover lithologies (McClenaghan et al. 2000, Forbes et al. accepted), while chemically transported pathfinder elements can be used in lithologies with a genetic link to the basement rocks (Lintern et al. 2006, Cheng 2014), or where past and present phreatic processes are understood (Aspandiar et al. 2008, Britt et al. 2010) . The nature and extent of pathfinder element mobilisation from basement mineralisation is not well understood across the Yorke Peninsula region, nor are the dispersion mechanisms associated with this movement.

In this study, whole rock geochemistry will be used to assess the cover sequence overlying mineralised and non-mineralised areas in the Yorke Peninsula region for pathfinder elements. The processes of chemical and mechanical transport of pathfinder elements through lithologies will then be assessed using qualitative elemental mapping and quantitative LA-ICP-MS analysis. A prospectivity index for basement mineralisation by Fabris et al. (2013) will be assessed and modified, concluding with a discussion on the criteria for exploration for IOCG type deposits in the Yorke Peninsula area using basal cover sequence lithologies.

BACKGROUND

The Yorke Peninsula in the southern Gawler Craton (Fig. 1) in South Australia hosts economic and sub-economic IOCG mineralisation including the historic Moonta-Wallaroo mining region and the Hillside deposit, hosted within Palaeoproterozoic basement rocks of the ca. 1750 Ma (Conor et al. 2010, Cowley et al. 2003) Wallaroo Group. The Wallaroo Group is comprised of three formations; the Wandearah Formation, the Matta Formation, and the Weetulta Formation. The Wandearah Formation contains the metasedimentary component of the Wallaroo Group, including clastic and chemical metasediments. The Matta Formation comprises mafic volcanics and amphibolite intrusives, and is interlayered with and locally intrudes the metasediments of the Wandearah Formation and the Weetulta Formation. The Weetulta Formation consists of felsic volcanics and subvolcanics of the Wallaroo Group (Cowley et al. 2003).

The Wallaroo Group has been variably metamorphosed from upper amphibolite facies in the south to greenschist facies in the north (Cowley et al. 2003, Conor 2002, Conor 1995). The Wallaroo Group has also undergone two phases of deformation: the earliest phase resulted in isoclinal folds and may have been associated with the ca. 1730-1690Ma (Hoek and Schaefer 1998, Hand et al. 2007) Kimban Orogeny, or during the early stages of the ca. 1600-1580 Ma event (Conor 2002). The second event resulted in upright folding and was associated with the ca. 1600-1580 Ma (Conor et al. 2010, Conor 2002) Tickera event, and intrusion of the Hiltaba Suite Granites, resulting in a period of intense hydrothermal magmatism. Metasomatism and mineralisation occurred at ~1600-1570Ma in association with the intrusion of the Hiltaba Suite Granites (Conor et al. 2010).

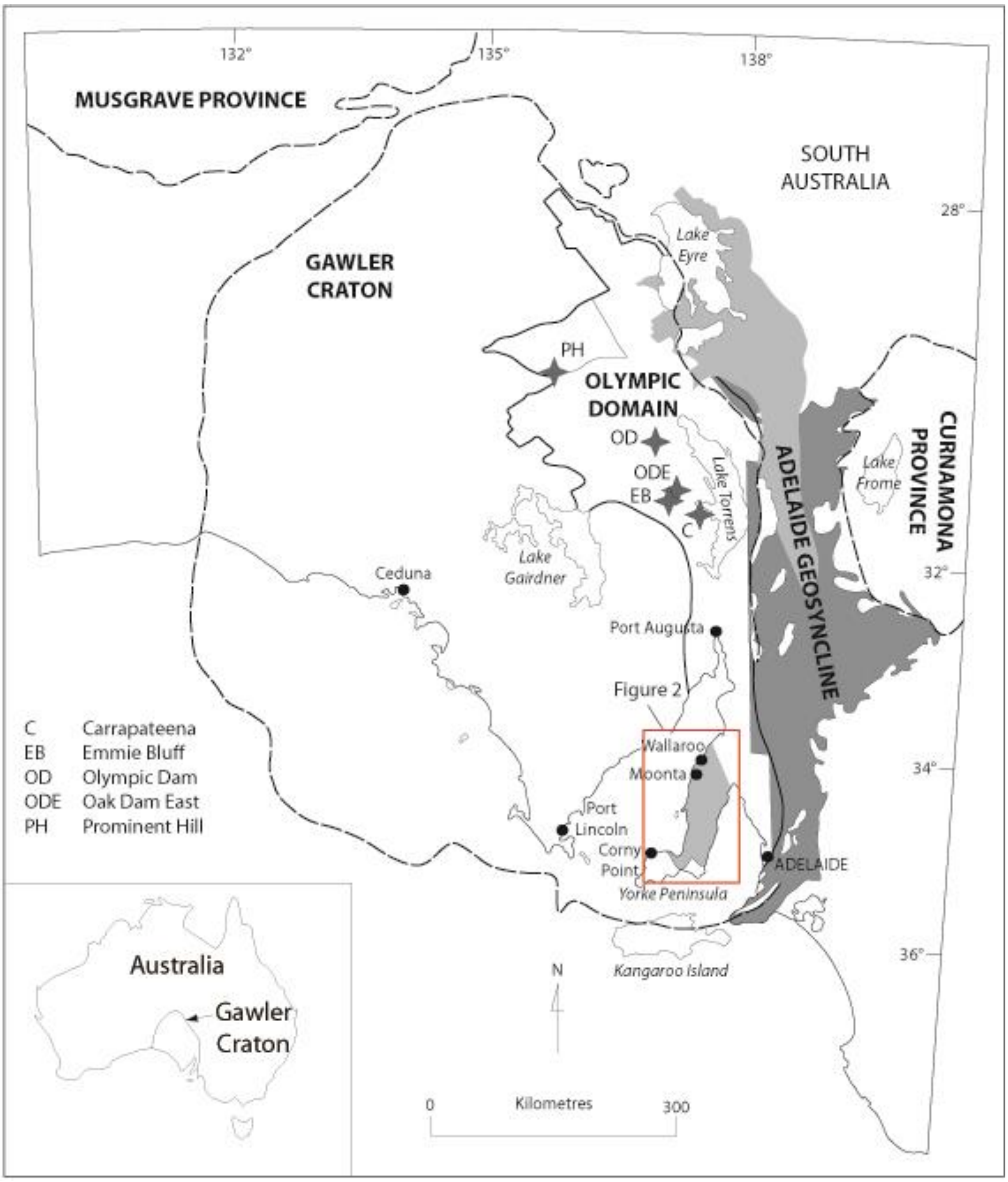

Figure 1: Geological map of the Gawler Craton showing major IOCG deposits within the Olympic Domain, South Australia, and the Yorke Peninsula study area. Modified from Forbes *et al* (accepted)

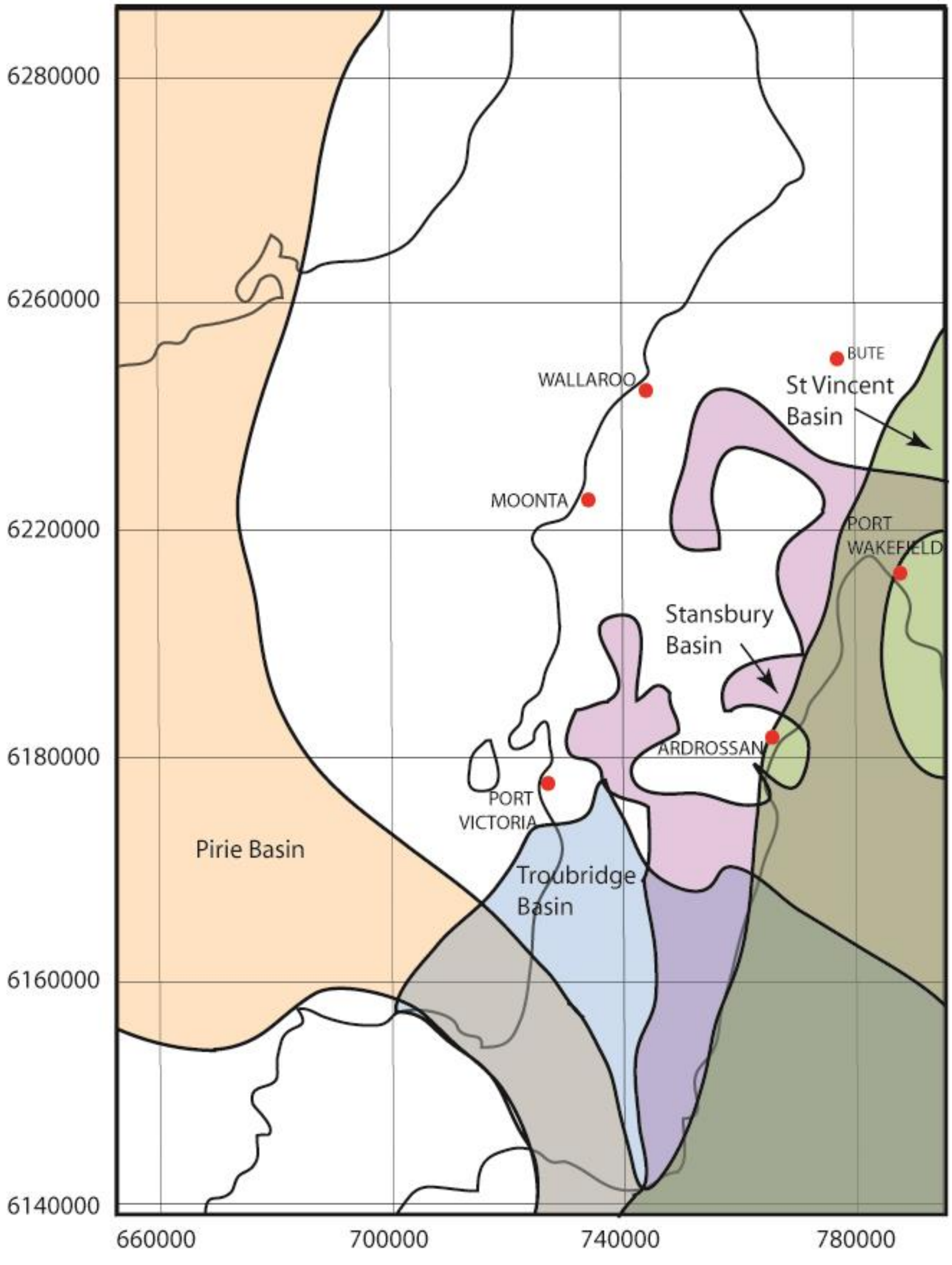

Figure 2: Geological map of the Yorke Peninsula showing the Pirie (Cambrian), Troubridge (Permian), St Vincent and Stansbury (Cenozoic) Basins. Map locality shown in Figure 1. Modified from Drexel & Preiss (1995).

The basement rocks in the Yorke Peninsula are extensively overlain by younger cover sequences that range from Neoproterozoic to Quaternary in age (Cowley et al. 2003). The Neoproterozoic lithologies unconformably overlie the basement rocks and have a composition that includes glacial diamictites and dolomitic limestone (Cowley et al. 2003). The Cambrian sediments of the Yorke Peninsula are encompassed within the Stansbury Basin, which covers an area of approximately 17,000 square kilometres and has a maximum thickness of 6km (Gravestock and Gatchouse 1995, Harvey and Hibburt 1999). This basin contains siliciclastic sediments, carbonate sediments, and sedimentary rocks (Daily 1990, Jago et al. 2002). The Permian Troubridge Basin (Fig. 2) overlies the Stansbury Basin, and has a maximum depth of 600m in glacially scoured valleys. On the Yorke Peninsula, the predominant Permian unit is the Cape Jervis Formation, a diamictite consisting of unconsolidated siltstone, sandstone, sandy limestone and grit, containing rounded pebbles, boulders and erratics. The Cenozoic St Vincent Basin (Fig. 2) is observed along the eastern edge of the Yorke Peninsula, and is composed of deltaic sediments overlain by younger marine sediments (Cowley et al. 2003, Jago et al. 2002). More than 90% of the Yorke Peninsula is covered by Quaternary sediments overlying the Stansbury and Troubridge basins (Fig. 2), and are likely to have been formed by glacio-eustatic sea-level oscillations (Zang 2003) .

METHODS

Logging and sampling

Sixty-nine open file drill holes across the central Yorke Peninsula (Fig. 3) were chosen for logging and sampling (Fig. 3). Drill holes were chosen based on whether they contained well preserved examples of the bottom of the cover sequence. Initial logging and sampling was undertaken in a Deep Exploration Technologies CRC (DET CRC) project in 2012, and reported in Forbes (2012).

The drillholes were originally logged to characterise the broad lithologies, and characteristics of particular interest included the composition and distribution of clast material in conglomerate and diamictite lithologies and evidence of alteration to the sediments, such as hematite banding and albitization. Additional detailed hand specimen analysis to further characterise the lithologies was undertaken in this study. The bottom one metre of logged cover sediments was sampled from each logged drill hole. Drill core samples were quarter or half core depending on availability. Drill hole details are given in Appendix A.

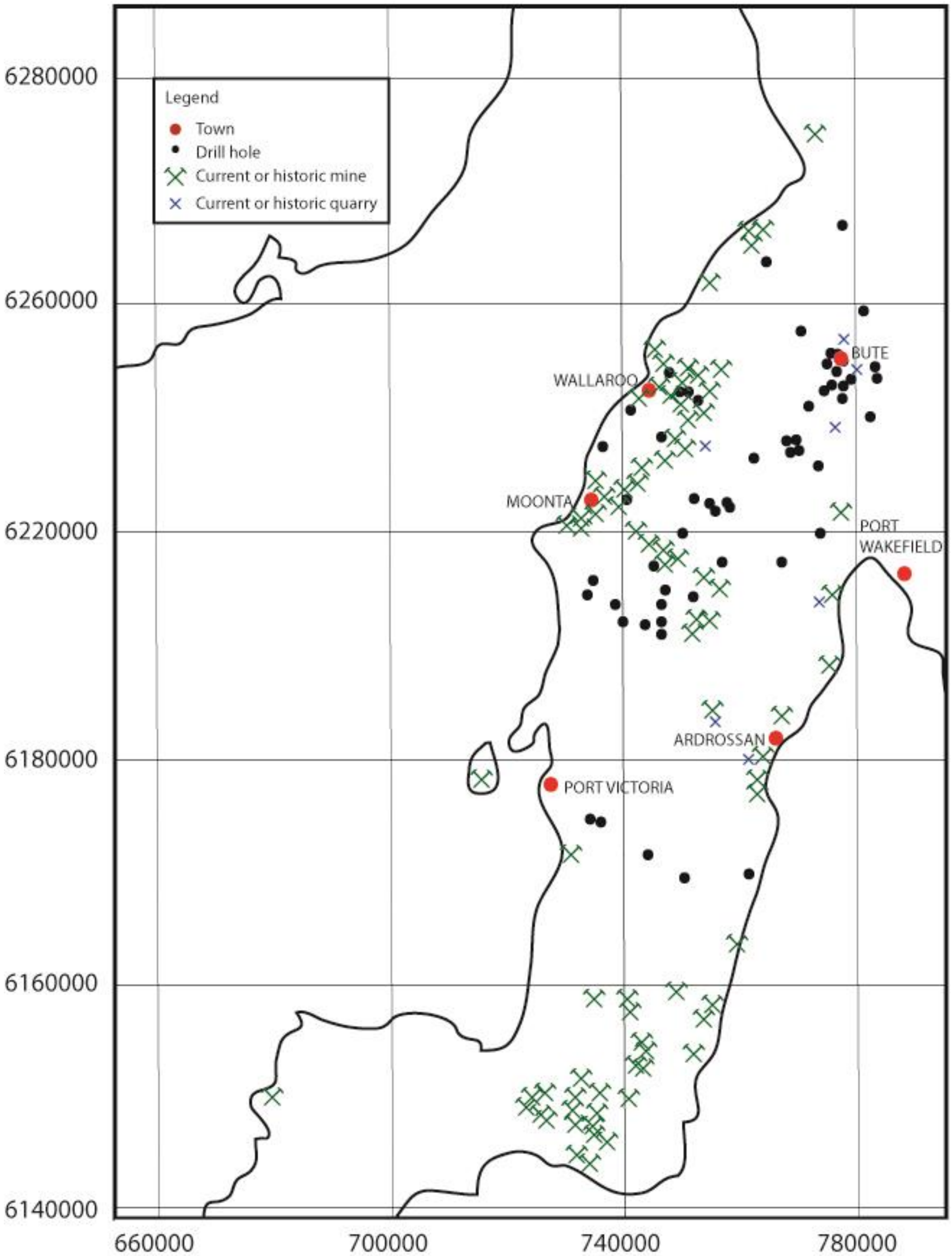

Figure 3: Map of Yorke Peninsula study area showing available and sampled drill holes and locations of historic and current mines and quarries.

Petrological analysis

Fourteen drill core samples were selected for thin section preparation. Ten centimetre sections were selected based on the presence of clasts (in the case of diamictites and conglomerates), veins and hematite alteration. Thin sections were prepared by Adelaide Petrographic Laboratories to a thickness of 30µm, and were used for petrological analysis by standard transmitted and reflected light microscopy to assess mineralogy and identify zones of alteration.

Geochemistry

Sample preparation and whole rock geochemical analysis of all remaining core was done by Genalysis Laboratories in Adelaide using standard ICP-OS and ICP-MS techniques. Gold was analysed by fire assay. Fluorine was analysed by carbonate fusion. Details of samples used is given in (Forbes 2012a, Forbes 2012b). Representative data is given in Tables 1 and 2. All data is given in Appendices B.

Elemental mapping

Six samples representative of the cover sequence lithologies and containing well preserved examples of sulphide mineralogy were chosen for qualitative elemental mapping to determine the nature of elemental distribution in samples and lithologies. Mapping was undertaken using a Philips XL30 Scanning Electron Microscope at Adelaide Microscopy, University of Adelaide. The maps were produced under conditions of 20.0kV and 95µA using a spot size of 5.000nm, dwell time of 250ns and a resolution of 512 x 400 pixels. Representative maps are shown in Figure 7. All maps are shown in Appendix C.

Mineral analysis

Quantitative mineral data was collected to determine the abundance of potential pathfinder elements within minerals of interest, particularly sulphides within varying textural environments. Mineral analysis was done using an Agilent 7500cx with attached New Wave UP-213 laser ablation system at Adelaide Microscopy, University of Adelaide. A laser fluence of 4.5J/cm^2, laser energy of 45%, repetition rate of 5Hz and spot size of 30µm were used. The concentration of Fe was set using stoichiometric concentrations within sulphide phases (59.8860wt% for pyrite). Representative data is given in Table 3. All data is given in Appendix D.

RESULTS

Logging

Five broad lithologies were identified within the basal cover sequence from detailed logging, including sandstones, clays, carbonates, diamictites and conglomerates. Where identifiable, lithological units have been broadly classified within the Yorke Peninsula cover sequence stratigraphy (Survey 1995). These lithologies are variably weathered and altered.

Sandstones include samples from the Emeroo Subgroup, Winulta Formation, and unidentified units (Unnamed Unit). Samples are very fine to medium grained (< ¼ mm – 1mm), and contain rounded to angular grains that are moderately to well sorted. Composition varies slightly, however all are composed predominantly of quartz and feldspar, with lesser plagioclase (up to 5%) and lithics (up to 10%). The sandstone cement is up to 25% of whole rock (Fig. 4a).

Clays are comprised of unidentified lithological units (Unnamed Unit), and are poorly consolidated to moderately lithified. The clays are very fine (< ¼ mm) to fine (½ - ¼ mm) grained. Subrounded to angular clasts of quartz, feldspar and calcrete, with lesser fragments of volcanics and weathered granite, potentially derived from the basement, are preserved within the clay. Clasts are up to ½ - 7mm size and comprise <10% of the whole rock.

Carbonates include samples from the Stansbury Limestone and unidentified units (Unnamed Unit) samples are predominately comprised of silty to sandy, finely laminated (<1mm) dolomitic carbonate. Laminations are composed of carbonate and silt/sand with carbonaceous cement layers. Some layers may contain sulphides in the form of pyrite. Limestone samples are non-fossiliferous (micrite), medium to coarse grained (1-2mm) and contain carbonate clasts that are irregular in shape and up to 10mm in size. These clasts occur in aggregates up to 5cm in size (Fig. 4b).

Diamictites include samples from the Sturt Tillite, Appila Tillite, and unidentified units (Unnamed Unit). Samples contain variable clast proportion (2-80% of whole rock). Clast and lithologies include quartz, feldspar, volcanics of felsic and mafic composition, carbonate, sandstone, siltstone, mudstone and lithics. Clasts are angular to rounded in shape and up to 50mm in diameter. The matrix is composed of very fine (< ¼ mm) to coarse (1 mm) grained sandstone. Late stage quartz stockwork veining overprints both matrix and clasts in some samples. Sulphides are present as both discrete small (<1mm) grains and at the boundaries of large clasts (Fig. 4c).

Conglomerates include samples from the Winulta Formation, Emeroo Subgroup, and unidentified units (Unnamed Unit). Samples contain variable clast proportion (5-80% of whole rock) and composition, with lithologies including quartzite, mudstone, granite, sandstone, mafics, volcanics, metasediments, and lithics. Clasts are subangular to rounded and >5mm. The matrix is very fine (<¼mm) to coarse (>1mm) grained sandstone, composed of rounded to subangular quartz (60 to >80% of matrix), feldspar (<20% of matrix) and cement (<5% of matrix). Lesser micaceous sandstone is also present as matrix. The matrix is often iron-stained. Quartz veins (up to 7mm wide) crosscut both matrix and clasts in some samples, comprising <5% whole rock. Sulphides are present along the boundaries of large clasts (Fig. 4d). Conglomerates can be distinguished from diamictites based on a higher clast proportion and evidence of bedding and/or foliations within some clasts.

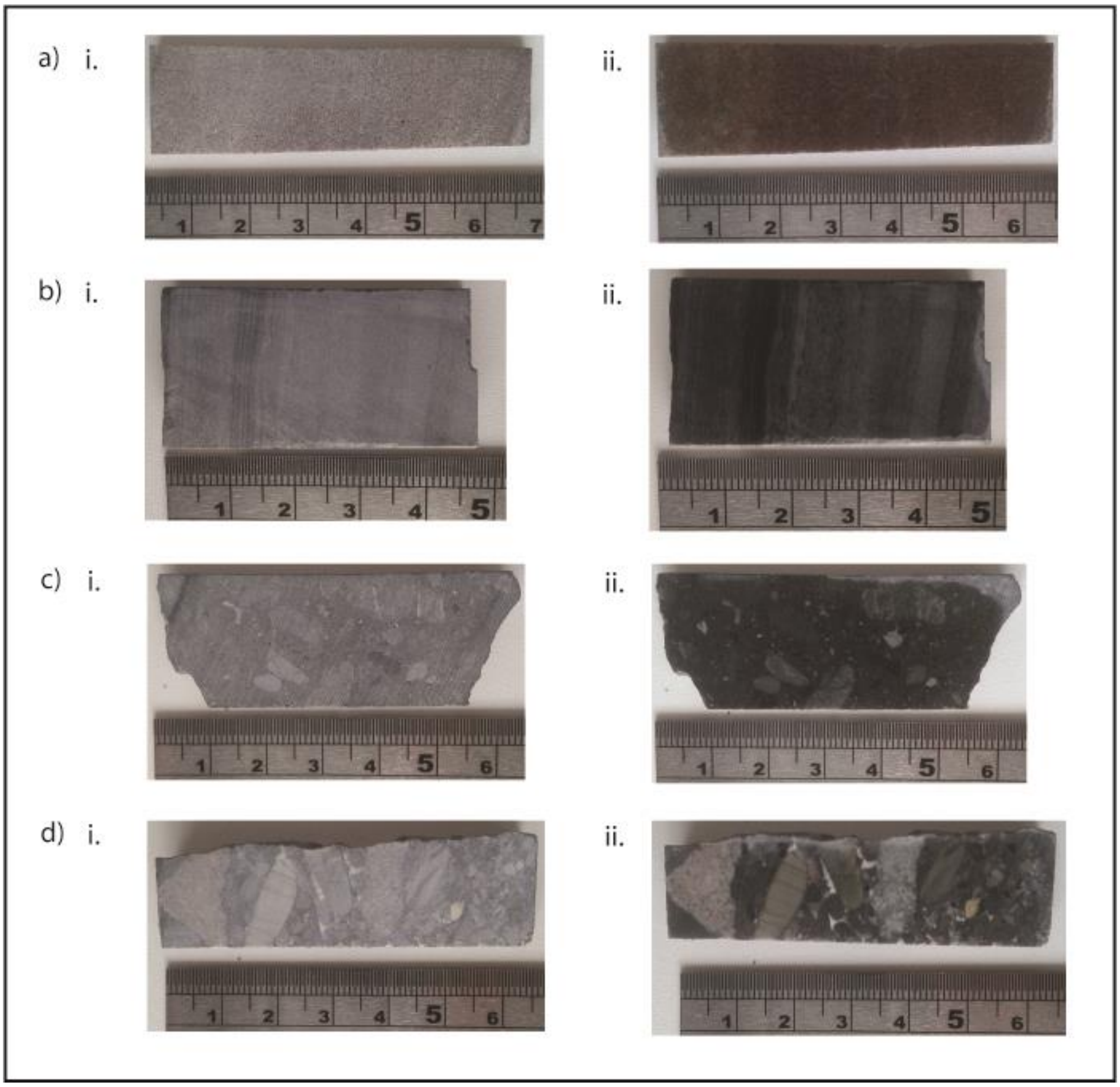

Figure 4: Representative thin section blocks of lithologies sampled; a) Sandstone i. dry, natural light, ii. wet, natural light; b) Carbonate i. dry, natural light, ii. wet, natural light; c) Diamictite i. dry, natural light, ii. wet, natural light; d) Conglomerate i. dry, natural light, ii. wet, natural light. Core samples for clay lithology were unavailable.

Whole rock geochemistry

Whole rock geochemical data was used to assess generic lithogeochemical characteristics of the broad lithologies identified in the logging, and to identify pathfinder elements towards potential IOCG mineralisation. Representative data is shown in Tables 1 and 2. Raw data is given in Appendix B.

MAJOR ELEMENT CHEMISTRY

Sandstone lithologies are characterised by high SiO_2 (>62wt%) and low MgO (<2wt%) and Fe (<7wt%) (Table 1). Clays show moderate SiO_2 (50wt% to 80wt%), moderate Al_2O_3 (<25wt%) and low MgO (<2wt%) and low Fe (<12wt%) (Table 1). Limestones and dolomitic carbonates are characterised by elevated CaO (>15wt%) and low Fe_2O_3 (<6wt%), K_2O (<1.5wt%) and Al_2O_3 (<5wt%) (Table 1). The carbonates can be further discriminated as limestones preserve the highest CaO (>35wt%) and low MgO (<1wt%), while dolomitic carbonates show lower CaO (15wt% - 30wt%) and high MgO (>12wt%) (Fig. 5).

The whole rock geochemistry of diamictites and conglomerates is dependent on clast and matrix composition and the modal proportion of clast versus matrix, and is therefore expected to be variable. The diamictite samples cluster on a MgO vs SiO_2 diagram (Fig. 5a), and have MgO content ranging from 1-5wt% and SiO_2 content ranging from 57-67wt% (Table 1). The diamictite samples show a positive linear relationship between CaO and MnO (Fig. 5c). The clustering of samples is due to the diamictites having similar clast and matrix composition and abundance.

The major element chemistry of conglomerate samples is more variable compared to the diamictites. The conglomerates are characterized by low Na_2O (<1wt%) (Table 1). Conglomerates can be separated into low MgO (<3wt%) and high MgO (>5wt%) groups, and display a negative linear relationship between MgO and SiO_2 (Fig. 5a) (Table 1). The whole rock chemistry of the conglomerate samples displays a higher degree of spread due to more variable clast composition and proportion of matrix.

Table 1: Major element chemistry from available drill holes, with averages of identified stratigraphic units shown along with overall lithological average, minimum and maximum.

Lith. Type	Strat. Name	Al_2O_3 (wt%)	CaO (wt%)	Fe_2O_3 (wt%)	K_2O (wt%)	MgO (wt%)	MnO (wt%)	Na_2O (wt%)	P_2O_5 (wt%)	SiO_2 (wt%)	TiO_2 (wt%)
Carbonates	Unnamed Unit	2.01	24.3	3.88	0.79	15.6	0.84	0.57	0.06	13.6	0.14
	Stansbury Limestone	4.40	37.8	1.09	1.33	0.80	0.11	1.59	0.04	23.2	0.15
	Average	2.39	26.0	3.88	0.79	13.7	0.84	0.57	0.06	14.8	0.14
	Minimum	0.81	19.2	1.09	0.23	0.87	0.11	0.05	0.01	4.45	0.07
	Maximum	4.40	37.8	5.93	1.33	17.7	1.21	1.59	0.13	29.9	0.17
Clay	Unnamed Unit	14.1	2.11	6.15	2.66	0.94	0.03	2.00	0.07	62.9	0.74
	Average	14.1	2.11	6.15	2.66	0.94	0.03	2.00	0.07	62.9	0.74
	Minimum	7.85	0.02	1.50	0.35	0.12	0.01	0.29	0.02	49.8	0.25
	Maximum	23.9	8.83	12.8	8.18	1.97	0.29	4.06	0.42	77.4	2.27
Conglomerate	Unnamed Unit	8.48	8.80	3.69	3.46	6.51	0.40	0.61	0.13	53.4	0.40
	Winulta Formation	5.41	1.99	3.93	2.70	1.40	0.04	0.33	0.10	81.1	0.22
	Emeroo Subgroup	10.8	0.44	7.02	4.54	2.13	0.06	0.10	0.18	70.2	0.85
	Average	6.67	2.33	4.47	3.10	1.99	0.08	0.31	0.12	76.6	0.35
	Minimum	2.30	0.03	2.03	1.42	0.10	0.01	0.04	0.01	53.4	0.07
	Maximum	12.4	10.6	8.01	5.83	6.51	0.40	0.93	0.29	93.7	0.91
Diamictite	Sturt Tillite	13.8	0.98	5.74	4.28	3.24	0.04	1.56	0.17	64.1	0.75
	Appila Tillite	12.6	2.90	5.70	4.29	4.13	0.16	1.35	0.18	61.4	0.72
	Unnamed Unit	11.1	1.57	6.16	3.54	2.02	0.07	2.26	0.14	71.5	0.66
	Average	12.4	2.32	5.82	4.10	3.49	0.12	1.60	0.17	64.3	0.71
	Minimum	6.83	0.58	3.01	3.03	0.97	0.01	0.10	0.12	57.9	0.34
	Maximum	15.4	4.61	9.30	4.85	4.88	0.30	4.42	0.22	82.8	0.98
Sandstone	Emeroo Subgroup	6.53	0.26	3.53	3.81	0.30	0.02	0.16	0.09	81.9	0.28
	Unnamed Unit	13.1	0.54	3.53	3.53	0.93	0.01	1.37	0.09	70.7	0.56
	Winulta Formation	4.17	0.96	4.08	2.51	0.32	0.01	0.52	0.19	86.4	0.16
	Average	10.4	0.52	3.60	3.35	0.81	0.01	0.96	0.10	75.5	0.44
	Minimum	4.17	0.04	1.89	1.09	0.35	0.01	0.12	0.02	63.1	0.16
	Maximum	17.2	1.75	5.32	4.49	1.87	0.03	3.23	0.20	86.4	0.85

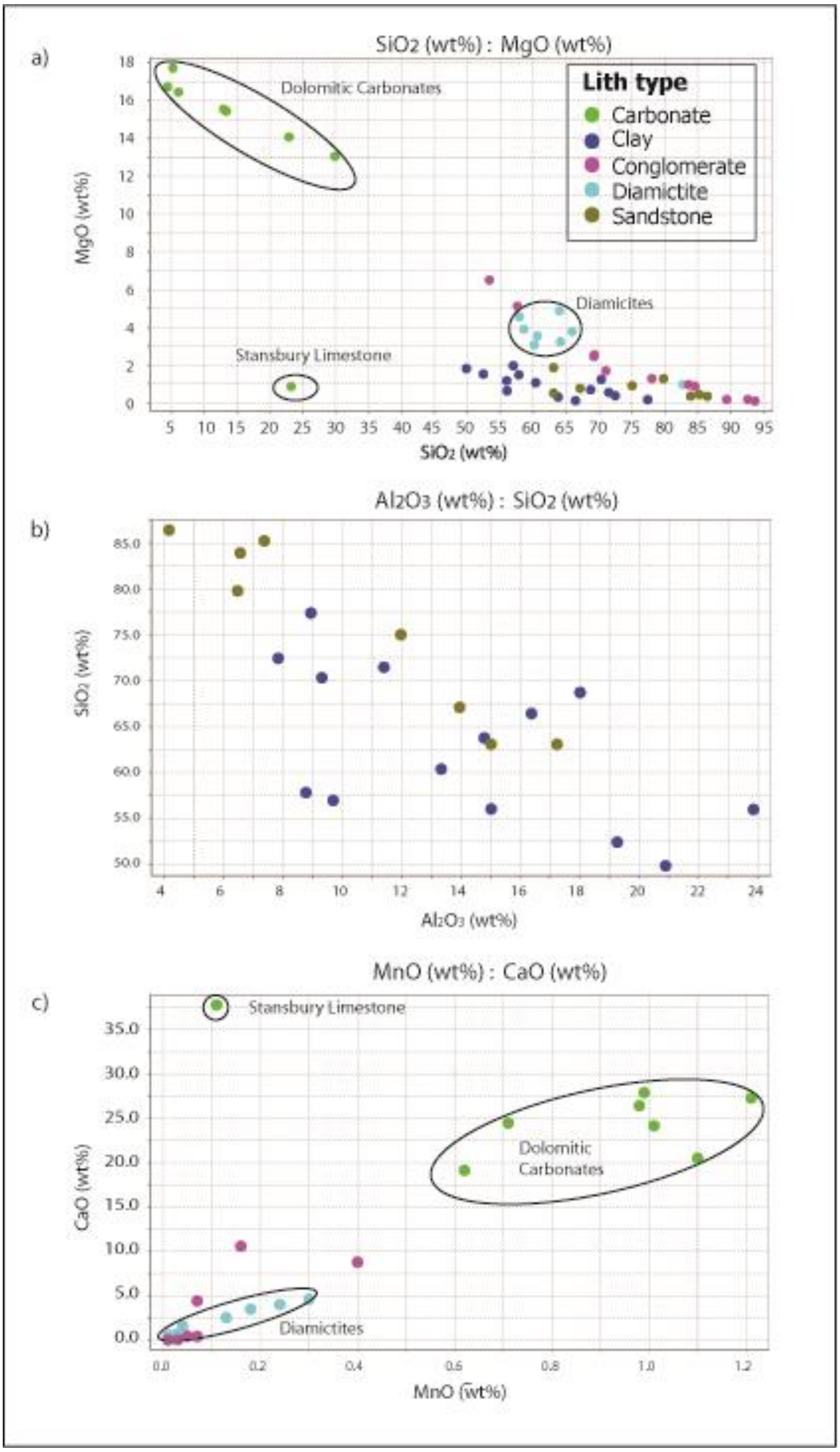

Figure 5: a) SiO2 v. MgO graph illustrating separation of carbonates from sediments and clustering of diamictite samples; b) Al2O3 v. SiO2 graph showing overlap of clay and sandstone lithologies; c) MnO v. CaO graph showing separation of dolomitic carbonates and limestone samples, positive linear trending of diamictite samples, and variability of conglomerate samples.

TRACE ELEMENT CHEMISTRY

Of particular interest to this study are the pathfinder elements related to potential IOCG mineralisation; Au, Ag, As, Bi, Co, Cu, Mo, S, Se, Sb, and W (Fabris et al. 2013, Mark et al. 2006) along with LREEs Ce and La. Representative data is shown in Table 2.

Sandstone lithologies have low measured values (less than 3x average crustal abundance) of Au (0.5 – 2ppb), Ag (0.025 – 0.2ppm), Bi (0.01 – 0.15ppm), Co (1.4 – 11.3ppm), Cu (8.0 – 76ppm) (Fig. 6b), Mo (0.1 – 1.5ppm) and Sb (0.09 – 0.34). Elements with elevated measured values (3 – 5x average crustal abundance include As (1.2 – 23.5ppm) (Fig. 6a). Elements with anomalous measured values (>5x crustal abundance) include Ce (31.5 – 1036.1ppm), La (19.3 – 513.5ppm) and Se (0.025 – 4.4ppm).

Clay lithologies preserve low measured values for Ag (0.025 – 0.49ppm) and Bi (0.005 – 0.45ppm). Elements with elevated measured values include Ce (6.4 – 212.4ppm), Co (1.1 – 69.4ppm), Cu (0.5 – 110ppm) (Fig. 6b), La (3.3 – 129.1ppm), Mo (0.4 – 5.1ppm), Sb (0.025 – 1.8ppm). Elements with anomalous measured values include Au (0.5 – 27ppb), As (0.5 – 61.5ppm) (Fig. 6a), and Se (0.025 – 6.1ppm).

Carbonate lithologies have low measured values for Au (0.5 – 3ppb), Ag (0.025 – 0.92ppm), Ce (15.1 – 75.7ppm) and La (8.1 – 35.2ppm). Elements with elevated values include Co (4.7 – 63.9ppm), Cu (57 – 602ppm), Mo (0.5 – 6.2ppm), Sb (0.08 – 1.79ppm). Anomalous values were measured for As (5.6 – 123.4ppm), Bi (0.01 – 1.54ppm), and Se (1.4 – 6.6ppm).

Diamictite samples have low values for Ag (0.025 – 1.08ppm), Ce (61.1 – 102ppm), La (29.6 – 52.7ppm) and Mo (0.3 – 1.9ppm). Elevated values were measured for Co (6.9 – 57.7ppm), Cu (19.0 – 571ppm) (Fig. 6b), Sb (0.23 – 1.95ppm). Anomalous values were measured for Au (0.5 – 235ppb), As (3.0 – 196.8ppm) (Fig. 6a), Bi (0.005 – 10.54ppm), and Se (0.025 – 7.4ppm).

Conglomerate samples contained low measured values for Ag (0.025 – 0.9ppm) and Mo (0.1 – 3.1ppm). Anomalous values were measured for Au (0.5 – 18ppb), As (2.0 – 318ppm) (Fig. 6a), Bi (0.005 – 1.01), Ce (27.7 – 489.5ppm), Co (1.1 – 118.8ppm), Cu (9.0 – 498ppm) (Fig. 6b), La (13.3 – 231.5ppm), Sb (0.17 – 3.29ppm) and Se (0.025 – 2.1ppm).

Table 2: Trace element chemistry of available drill holes, with averages of identified stratigraphic units shown along with overall lithological average, minimum and maximum. Average crustal abundance taken from Rudnick and Gao (2004)

	Stratigraphic Name	Au (ppb)	Ag (ppm)	As (ppm)	Bi (ppm)	Ce (ppm)	Co (ppm)	Cu (ppm)	La (ppm)	Li (ppm)	Mo (ppm)	Ni (ppm)	S (ppm)	Sb (ppm)	Se (ppm)	U (ppm)	W (ppm)	Zn (ppm)
Carbonate	Unnamed unit	0.86	0.49	58.8	0.50	34.6	28.3	249	17.8	4.37	2.60	10.4	5187	0.79	3.40	2.48	0.60	37.4
	Stansbury LS	0.50	0.92	32.0	0.07	23.4	11.4	303	12.0	1.40	4.50	2.00	4312	1.23	4.00	5.86	0.05	35.0
	Average	0.81	0.54	55.5	0.44	33.2	26.3	256	17.1	4.00	2.84	9.38	5078	0.85	3.48	2.90	0.53	37.1
	Minimum	0.50	0.03	5.60	0.01	15.1	4.70	46.0	7.80	1.40	0.50	1.00	25.0	0.08	1.40	1.80	0.05	19.0
	Maximum	3.00	0.77	123	1.54	75.7	63.9	602	35.2	6.90	6.20	256	12973	1.79	6.60	2.35	2.00	63.0
Clay	Unnamed unit	2.39	0.09	11.6	0.12	60.9	12.5	44.9	33.7	15.0	1.54	16.9	355	0.55	2.69	3.57	4.80	40.2
	Average	2.39	0.09	11.6	0.12	60.9	12.5	44.9	33.7	15.0	1.54	16.9	355	0.55	2.69	3.57	4.80	40.2
	Minimum	0.50	0.03	0.50	0.01	6.40	1.10	0.50	3.30	2.40	0.40	0.05	75.0	0.03	0.03	1.18	0.05	4.00
	Maximum	27.0	0.49	61.5	0.45	212	69.4	110	129	43.9	5.10	64.0	785	1.80	6.10	7.21	34.0	132
Conglomerate	Unnamed unit	2.00	0.90	318	0.24	42.4	119	145	21.3	25.6	3.10	59.1	9657	3.29	0.03	2.60	5.00	13.0
	Winulta Form.	0.70	0.08	8.04	0.06	127	4.70	112	60.9	17.6	0.50	15.0	206	0.28	0.52	3.60	1.40	38.8
	Emeroo S.G	17.0	0.06	7.65	0.63	108	11.4	20.0	57.6	34.9	0.40	29.0	163	0.63	1.06	4.50	24.0	116
	Average	3.68	0.15	36.1	0.18	116	16.3	98.0	56.7	21.4	0.72	21.1	1057	0.61	0.57	3.66	5.73	50.5
	Minimum	0.50	0.03	2.00	0.01	27.7	1.10	9.00	13.3	4.30	0.10	0.05	25.0	0.17	0.03	1.11	0.05	0.05
	Maximum	18.0	0.90	318	1.01	490	119	498	232	40.3	3.10	59.0	9657	3.29	2.10	7.49	26.0	145
Diamictite	Sturt Tillite	2.00	0.07	22.6	0.38	102	16.5	61.0	52.0	69.7	1.10	25.0	968	0.37	0.03	3.60	3.00	92.0
	Appila Tillite	2.00	0.36	62.0	3.37	81.6	27.8	221	42.1	54.7	1.26	35.0	2678	1.23	2.89	3.80	4.40	45.2
	Unnamed unit	118	0.03	4.01	0.02	80.0	15.0	26.1	42.9	23.9	0.30	33.0	514	0.26	0.03	3.90	4.50	140
	Average	30.9	0.24	42.6	2.16	83.7	23.2	152	43.5	48.9	1.00	33.4	1923	0.88	1.82	3.79	4.25	74.6
	Minimum	0.50	0.03	3.00	0.01	61.1	6.90	19.0	29.6	18.6	0.30	18.0	346	0.23	0.03	2.87	2.00	23.0
	Maximum	235	1.08	197	10.5	102	57.7	571	52.7	73.7	1.90	48.0	5847	1.95	7.40	6.00	7.00	209
Sandstone	Unnamed unit	0.50	0.08	5.64	0.09	292	5.68	25.2	143	18.2	0.84	11.0	168	0.34	2.90	8.50	2.80	44.4
	Emeroo S.G	1.30	0.09	15.3	0.07	72.0	4.30	44.0	38.6	15.1	0.45	4.50	223	0.31	3.15	3.10	4.00	25.5
	Winulta Form.	0.50	0.03	6.00	0.01	129	11.3	63.0	56.5	6.50	1.50	66.0	104	0.18	0.03	5.60	3.00	7.00
	Average	0.69	0.08	8.10	0.07	217	6.04	34.1	106	15.9	0.82	16.5	174	0.31	2.60	6.76	3.13	35.0
	Minimum	0.50	0.03	1.20	0.01	31.5	1.40	8.00	19.3	6.10	0.10	2.00	86.0	0.09	0.03	1.26	0.05	7.00
	Maximum	2.00	0.20	23.5	0.15	1036	11.3	76.0	514	23.6	2.00	66.0	361	0.80	4.40	19.3	6.0	101
Average Upper Crustal Abundance*		1.50	0.05	4.80	0.16	63.0	17.3	28.0	31.0	24.0	1.10	47.0	62.0	0.40	0.09	2.70	1.90	67.0

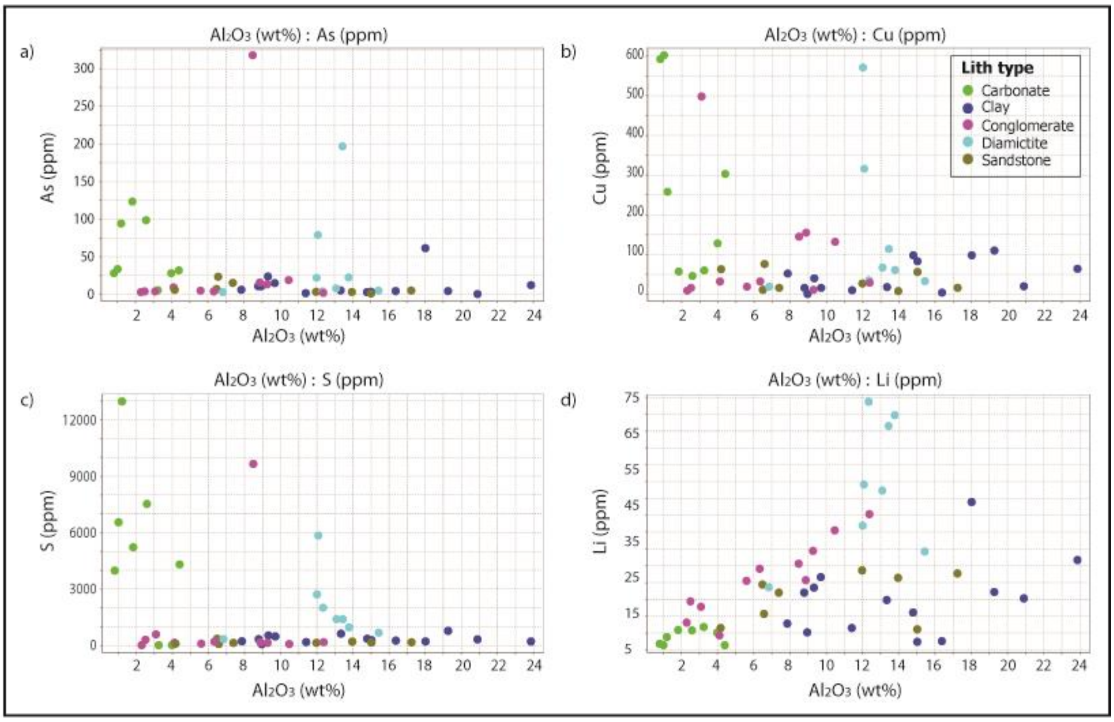

Figure 6: Variations in trace element chemistry; a) Al2O3 (wt%) v. As (ppm) graph showing outliers from carbonate, conglomerate, diamictite and clay lithologies demonstrating potential enrichment of As; b) Al2O3 (wt%) v. Cu (ppm) graph showing potential enrichment of Cu in samples from the carbonate, conglomerate and diamictite lithologies; c) Al2O3 (wt%) v. S (ppm) showing enrichment in carbonate lithology, indicating a potential lithological feature rather than potential enrichment; d) Al2O3 (wt%) v. Li (ppm) showing slightly elevated Li as a potential lithological feature of diamictites, with no other clear outlying values to illustrate enrichment.

Elemental mapping and back-scatter electron (BSE) imaging

Qualitative elemental mapping and BSE imaging were done on samples that were identified to preserve elevated concentrations of trace elements that may be potential pathfinders towards IOCG mineralisation. The areas imaged were selected to target sulphides and identify light rare earth element (LREE) hosts.

Representative element maps are shown in Figure 7. All element maps are shown in Appendix C. Elemental mapping shows that the samples are predominantly composed of quartz (elevated Si), with lesser feldspar (elevated Al, K, Si, Na) and carbonates (elevated Mg, Ca, no S). Sulphides identified were pyrite (elevated Fe and S) and chalcopyrite (elevated Cu, Fe and S) (Fig. 7c). Sulphides can be further discriminated by their grain shape, size and textural relationship with clast as either primary (Fig. 7a) or remobilised (Fig. 7c) sulphides. Primary sulphides are present as small, discrete grains (up to 20µm) and occur within the matrix of diamictite samples (Fig. 7a).

Remobilised sulphides are more abundant than primary sulphide grains, and are present along clast boundaries within the conglomerate sample. Remobilised pyrite was observed to coexist with chalcopyrite, identifiable by abundance of copper (Fig. 7c). Low level enrichment of cobalt is observed in small sections of pyrite (Fig. 7c). No other trace elements or LREEs were detectable in secondary sulphides.

BSE imaging was used to identify LREE hosts. A representative image is shown in Figure 7d. LREEs were identified within small (<15µm) grains of monazite within a diamictite matrix. The grains are angular to subangular in shape and occur in groups of 5-10 grains throughout the matrix (Fig. 7d).

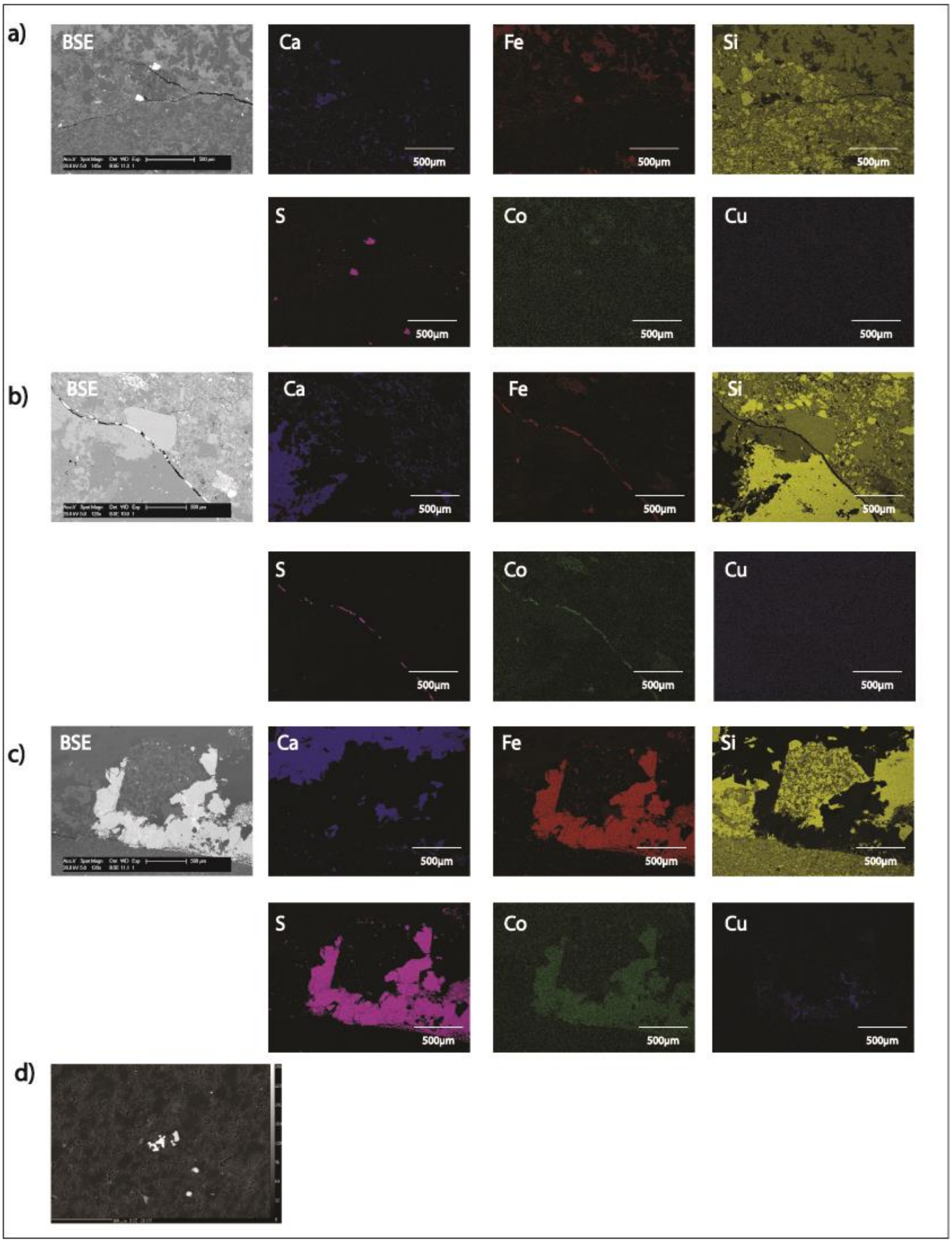

Figure 7: Selected qualitative element maps showing back scatter electron images (BSE), Ca, Fe, Si, S, Co and Cu content; a) Sulphide grains present in a quartz, feldspar and dolomite rich matrix of a diamictite; b) Sulphide grains present within a vein through quartz and dolomite within a diamictite sample; c) Sulphides present around the boundary of quartz grains, with coexisting chalcopyrite, in a conglomerate sample; d) BSE image of monazite grains within the matrix of a diamictite sample.

Mineral chemistry

LA-ICP-MS spot analysis of pyrite and chalcopyrite was undertaken from one diamictite and one conglomerate sample. Results are summarised in Table 3 and given in Appendix D. The diamictite sample contains primary sulphides, while the conglomerate sample contains remobilised sulphides. Chalcopyrite grains were not analysed as the grains were too small. The concentrations of IOCG pathfinder elements were measured.

Table 3: LA-ICP-MS data for analysed samples, including average for lithologies.

Lith. Type	Sample	Au (ppm)	Ag (ppm)	As (ppm)	Bi (ppm)	Co (ppm)	Cu (ppm)	Mo (ppm)	Ni (ppm)	Sb (ppm)	Se (ppm)	W (ppm)	Zn (ppm)
Diamictite	016_101	0.000	3.394	685.5	3.737	2072	748.9	0.364	374.9	5.596	22.82	0.000	0.000
	016_102	0.163	3.500	3352	10.63	1559	804.7	1.100	171.6	5.670	18.95	0.340	54.57
	016_103	0.101	6.524	301.2	11.36	1567	1117	1.321	205.8	13.39	0.000	1.409	61.97
	016_104	0.076	17.15	722.5	15.19	1098	1900	10.85	429.2	10.62	14.61	2.200	8.950
	016_105	0.000	2.033	499.2	17.42	1184	299.1	2.750	1068	5.502	52.48	2.183	1051
	016_201	0.044	5.192	201.9	59.06	675.6	177.4	16.96	1363	6.719	17.42	0.000	1.293
	016_202	0.000	4.377	113.2	47.27	591.2	94.35	5.969	1414	3.429	13.00	0.209	0.000
	016_203	0.069	14.52	304.8	63.40	788.8	2574	11.59	1446	6.415	19.29	1.283	17.79
	016_204	0.092	16.64	166.7	57.67	720.0	133.9	8.693	1723	7.404	33.39	0.625	7.726
	016_205	0.064	8.134	117.0	49.13	743.2	124.8	5.359	2006	4.629	39.61	0.215	3.637
	016_206	0.058	3.637	76.13	12.85	354.7	48.48	1.001	774.5	1.675	15.62	0.000	2.002
	Average	**0.060**	**7.740**	**595.0**	**31.60**	**1032**	**729.0**	**6.000**	**998.0**	**6.460**	**22.50**	**0.800**	**109.9**
Conglomerate	882_101	0.000	27.46	3920	2.372	2088	429.1	12.87	1344	42.85	0.000	4.346	45.16
	882_102	0.000	20.65	3787	0.284	1658	338.1	7.482	1147	41.48	0.000	5.392	31.66
	882_103	0.000	12.33	3065	0.240	1764	147.3	8.599	1333	34.28	0.000	9.557	14.12
	882_104	0.000	10.43	2694	0.235	1849	70.63	4.825	1352	26.90	0.000	5.101	16.15
	882_201	0.000	12.95	1213	0.000	7.963	251.1	2.515	11.09	490.9	0.000	0.000	1.850
	882_202	0.000	20.01	2404	0.150	63.62	435.2	29.66	41.92	498.1	0.000	0.000	1.877
	882_203	0.000	17.32	6849	0.272	54.22	274.0	17.66	32.96	320.9	0.000	0.000	1.729
	882_204	0.000	9.625	17013	0.537	14.78	27.53	8.848	9.376	25.29	0.000	0.000	0.000
	882_205	0.000	9.670	13676	0.000	1.642	6.768	4.230	1.476	16.10	0.000	0.000	1.299
	882_211	0.000	9.135	12449	0.339	15.77	21.31	10.73	15.83	10.08	0.000	0.000	3.967
	882_212	0.000	11.48	13547	1.591	89.65	168.3	13.88	38.36	40.13	0.000	0.050	5.055
	882_213	0.000	13.70	15683	0.470	32.94	42.93	30.60	13.05	35.72	0.000	0.000	1.412
	882_214	0.000	13.53	17499	0.258	29.30	108.1	17.10	8.788	41.82	0.000	0.000	2.302
	882_215	0.000	7.948	3257	0.322	199.3	255.7	60.20	87.75	493.7	0.000	0.000	0.000
	882_216	0.000	16.95	19260	0.151	4.344	7.997	13.73	8.389	60.85	0.000	0.000	0.000
	882_217	0.000	11.66	17294	0.000	3.823	23.00	34.65	4.433	39.79	0.000	0.000	2.562
	882_218	0.000	12.16	7143	0.025	14.41	66.98	21.97	12.30	74.52	0.000	0.000	0.000
	882_219	0.000	16.46	4691	0.124	50.88	457.7	30.10	28.76	665.6	0.000	0.064	0.000
	882_220	0.000	13.31	8218	0.903	61.21	26.06	27.33	23.42	14.01	0.000	0.000	2.024
	882_221	0.000	33.44	2479	1.049	92.43	547.2	4.133	42.38	851.4	0.000	0.000	0.000
	Average	**0.000**	**15.00**	**8807**	**0.470**	**405.0**	**185.0**	**18.10**	**278.0**	**191.0**	**0.000**	**1.200**	**6.558**

DIAMICTITE

The diamictite sample had higher measured values for cobalt (average 1032.0ppm), nickel (average 998ppm), and copper (average 729.0ppm), and lower measured values for antimony (average 6.646pm) and arsenic (average 595.0ppm) than the conglomerate sample. Moderate values were measured for bismuth (average 31.60ppm) and silver (average 7.70ppm). Concentrations of gold (<0.2ppm) and tungsten (<10ppm) were extremely low (Table 3)

CONGLOMERATE

The conglomerate samples contained higher measured values for antimony (average 191.0ppm) (Fig. 8c) and arsenic (average 8807ppm), and lower values for nickel (average 278.0ppm) (Fig. 8e) and cobalt (405.0ppm) (Fig. 8d) than measured in the diamictite sample. Moderate values were measured for silver (7.82 – 32.53ppm) and copper (6.88 – 532.35ppm). Low measured values were recorded for gold (<0.2ppm), tungsten (<10ppm) and bismuth (<1.02ppm).

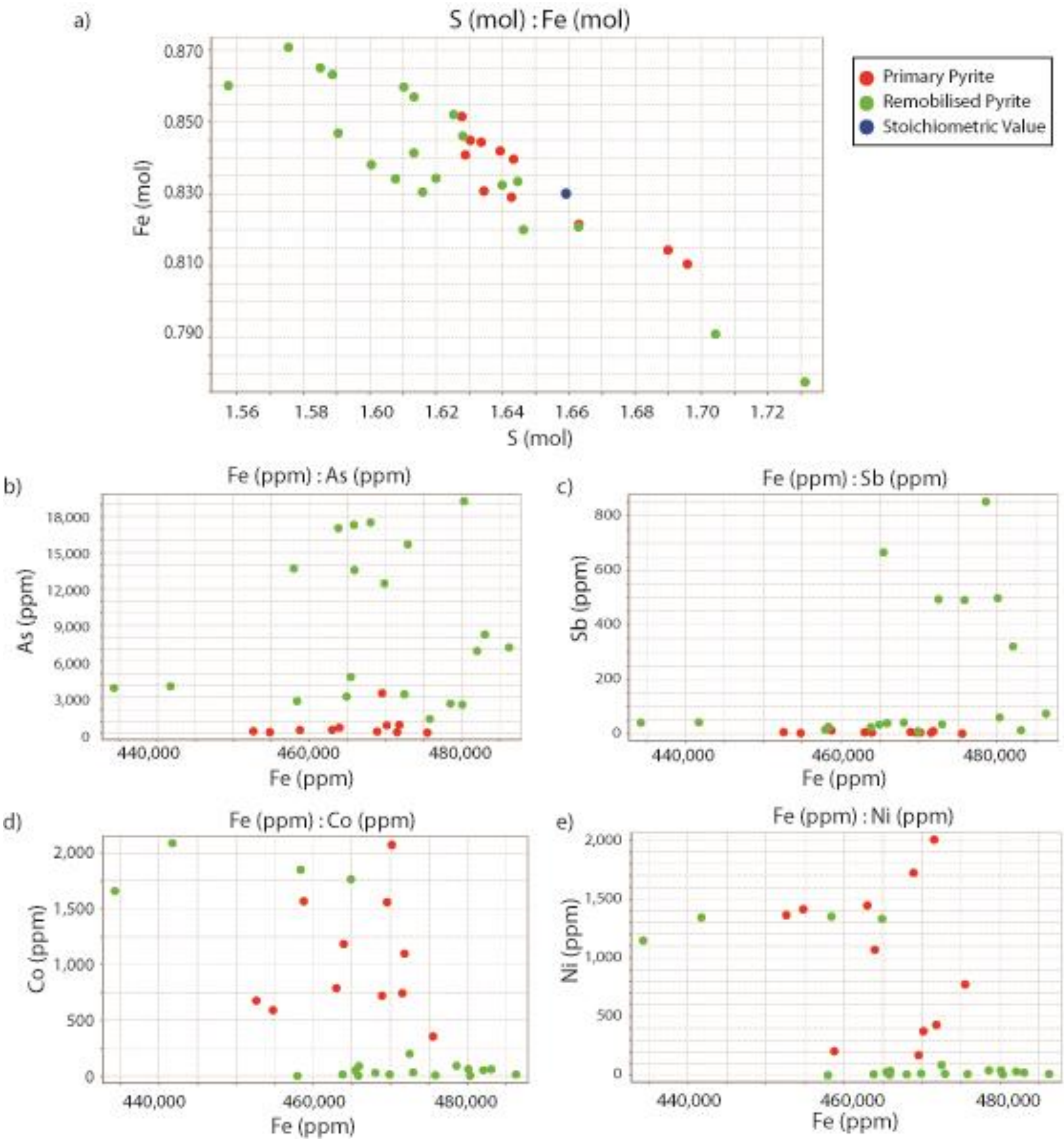

Figure 8: LA-ICP-MS data for pyrite samples; a) S (mol) v. Fe (mol) graph showing primary and remobilised sulphide samples, with stoichiometric value for pyrite included; b) Graph of Fe (ppm) v. As (ppm) showing elevation of As within remobilised pyrite samples compared to primary pyrite samples; c) Graph of Fe (ppm) v. Sb (ppm) showing elevation of Sb within remobilised pyrite samples; d) Graph of Fe (ppm) v. Co (ppm) showing elevation of Co predominantly within primary pyrite samples; e) Graph of Fe (ppm) v. Ni (ppm) showing elevation of Ni predominantly within primary pyrite samples.

DISCUSSION

Geochemical characterisation of cover lithologies

In order to determine the background chemistry of samples and to normalise all lithological data to a single element, it is important to characterise the geochemistry of individual lithologies. This allows anomalous concentrations of elements within lithologies to be correctly identified, including those of potential use as vectors towards IOCG mineralisation.

The Yorke Peninsula basal cover sequence lithologies are best discriminated on a MgO vs SiO_2 diagram (Fig. 9a, b). Carbonates are clearly discriminated based on their high MgO and low SiO_2 content. The diagram shows a negative linear trend in the conglomerate lithology, and also separates these samples into a low MgO/high SiO_2 group and a high MgO/low SiO_2 group. Diamictites group between 3.0 – 5.0% MgO and 57.0 – 67.0% SiO_2. The carbonates themselves can be further discriminated as dolomitic carbonates and limestones based on their CaO and MgO content (Fig. 9f) Sandstone and clay lithologies are not able to be reliably differentiated through geochemistry alone as they have similar geochemistry, however they can be divided into three groups: a clay endmember, a sand endmember, and a clay/sand mix (Fig. 9c,e). Low-Mg conglomerates are also difficult to distinguish as they also overlap geochemically with the sandstone lithology (Fig. 9e). Diamictites can be separated from sandstones and clays as they have high MnO and MgO content (Fig. 9d)

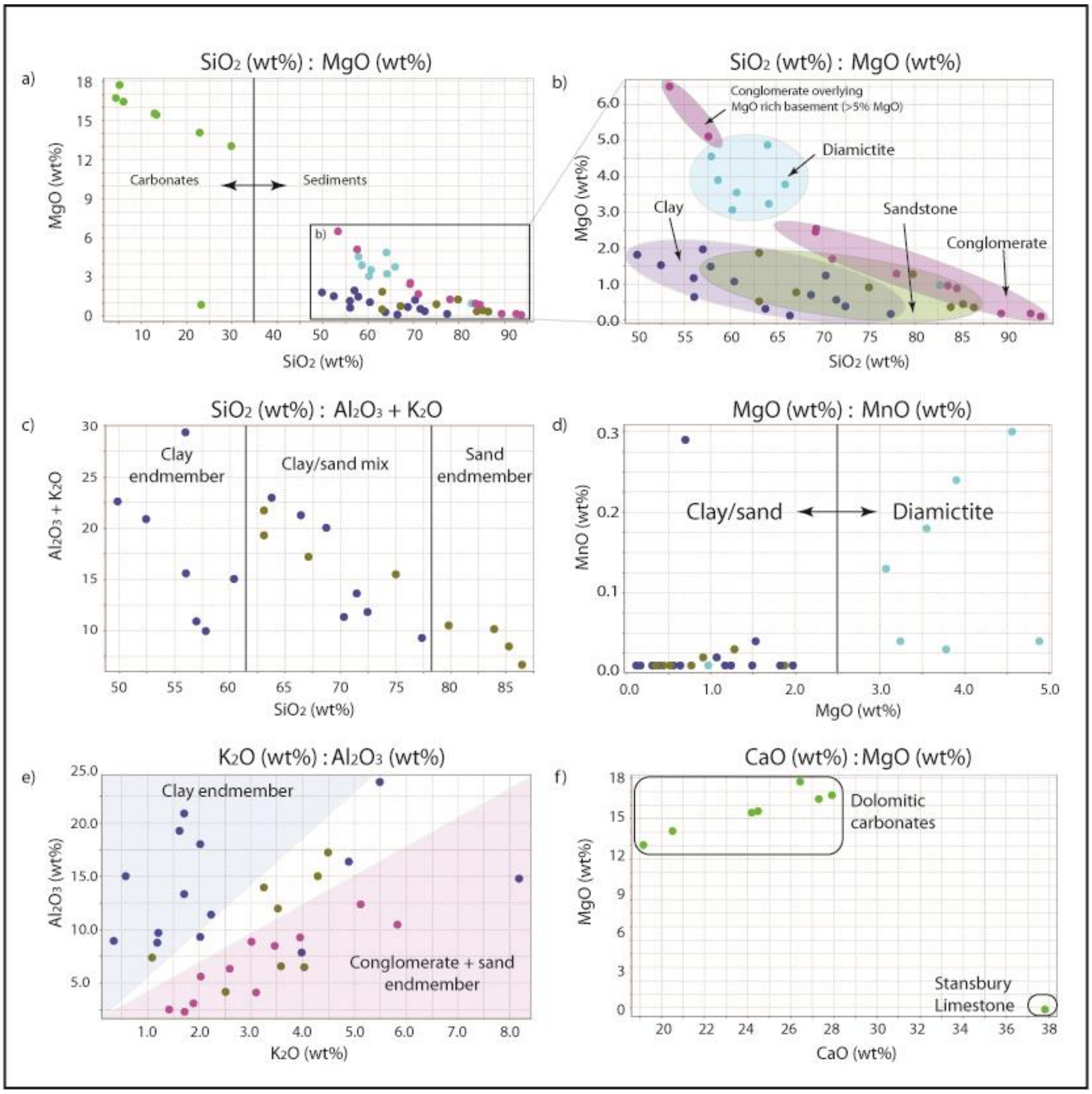

Figure 9: Lithogeochemical workflow demonstrating the methods of determination of lithologies based on their whole rock geochemistry; a) Data from all lithologies on SiO_2 v. MgO graph used to separate carbonaceous lithologies from sediments; b) Graph of SiO_2 v. MgO with carbonaceous lithologies removed, illustrating grouping of lithologies by geochemistry, as well as substantial overlap of lithologies; c) SiO_2 v. Al_2O_3 + K_2O graph showing sandstone and clay lithologies as endmembers rather than separate lithologies, with an area of mixed composition between the two endmembers; d) MgO v. MgO graph used to separate diamictite lithology from clays and sandstones; e) K_2O v. Al_2O_3 graph showing overlap of conglomerate lithology and sandstone endmember, illustrating the difficulty separating these lithologies geochemically; f) CaO v. MgO graph used to separate dolomitic carbonates from limestones.

Pathfinder elements for potential IOCG mineralisation

The whole rock element suite was assessed for pathfinder elements, with emphasis placed on elements with known associations with IOCG mineralisation (Au, Ag, As, Bi, Ce, Co, Cu, La, Mo, S, Se, Sb, and W (Fabris et al. 2013, Mark et al. 2006)). However, as average trace element concentration will naturally vary between lithologies (Scott and Pain 2008) the Yorke Peninsula cover sequence lithologies can only be compared to one another after normalisation of the whole rock data.

As the cover sequence lithologies across the Yorke Peninsula can be broadly discriminated using SiO_2 (Fig. 9), this element was used to normalise the whole rock geochemical data for the sediments (clay, sandstone, conglomerate and diamictite). Normalisation of data for the carbonates and carbonaceous sediments resulted in the data becoming heavily skewed, therefore these lithologies were excluded from normalisation with SiO_2. Normalisation with MgO is more appropriate for carbonates and carbonaceous sediments, however the type of carbonate must be determined before the data can be used. Marine carbonates are not genetically linked to the basement rocks and therefore do not preserve elemental signatures related to basement mineralisation, while pedogenic carbonates have been successfully used to explore for various commodities within Australia (Lintern et al. 2006, Lintern 2014, McQueen et al. 1999). It is difficult to distinguish between marine and pedogenic carbonates (Lintern 2014), therefore these samples were excluded from the dataset.

Pathfinder elements within the Yorke Peninsula cover sequence that may be used to vector towards potential IOCG mineralisation were assessed using normalised histograms and probability plots shown in Figure 10. Elements that were identified to be potential pathfinders include As, Co, Sb, Cu, Au, Ce and La, while elements such as Te, Se, Mo, Ag, U and Bi were below level of detection.

Normalised histograms have had a log transformation applied as the trace element data presents as a lognormal distribution (McQueen 2006). The following elements were found to show anomalous concentrations from the normalised histograms; Sb, As, Co and S (Fig. 10). Probability plots (also normalised against SiO_2) allow background concentrations of trace elements to be statistically determined and anomalous data to be identified with relative ease.

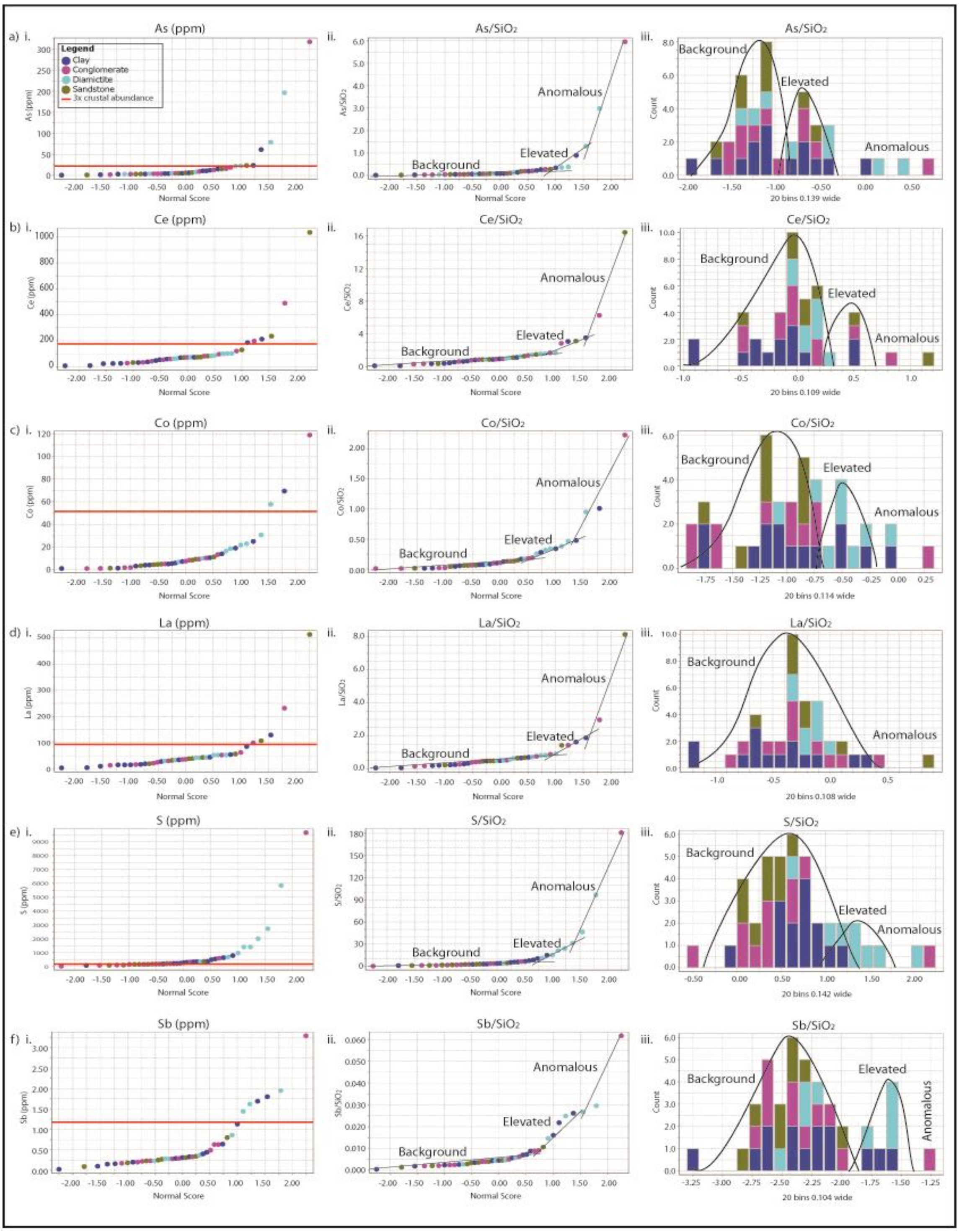

Figure 10: Probability plots with 3x average crustal abundance shown of a)i. As; b)i. Ce; c)i. Co; d)i. La; e)i. S; f)i. Sb. Normalised probability plots showing background, elevated and anomalous data of a)ii. As/SiO$_2$; b)ii. Ce/SiO$_2$; c)ii. Co/SiO$_2$; d)ii. La/SiO$_2$; e)ii. S/SiO$_2$; f)ii. Sb/SiO$_2$. Normalised histograms with log transformation applied showing background, elevated and anomalous data for a)iii. As/SiO$_2$; b)iii. Ce/SiO$_2$; c)iii. Co/SiO$_2$; d)iii. La/SiO$_2$; e)iii. S/SiO$_2$; f) Sb/SiO$_2$.

Element deployment

Stoichiometric values for pyrite were used to compare the data collected. Deviation of Fe and S from the stoichiometric value indicate space for substitution of trace elements into the pyrite (Fig. 8a).

Cobalt and nickel occur together in primary grains of pyrite (Fig. 8), and are known to commonly occur within pyrite (Nishiyama 1983, Huston et al. 1995). Selenium and tellurium occur together in the diamictite samples at greater concentration than in the conglomerate sample, and have been known to occur as stoichiometric substitutions for sulphur in pyrite (Huston et al. 1995), however the concentrations of Se and Te are low compared to levels expected in other sulphide minerals, such as bornite and chalcocite (Cook et al. 2011), and it is likely that Se and Te will preferentially partition into these minerals where they coexist with pyrite. Preferential partitioning of elements into other sulphide minerals accounts for anomalous values for trace elements within the whole rock data, and comparatively low concentrations within pyrite grains. As fluid-assisted remobilisation of elements does not commonly result in the movement of these elements (Cook et al. 2013) this suggests that these grains may not have experienced remobilisation by fluids, and therefore are likely to have been mechanically transported into the cover sequence.

Antimony and arsenic occur within the conglomerate sample, however they occur separately (Fig. 10b,d), indicating preferential substitution of one or the other. Arsenic is a common substitution in pyrite grains (Huston et al. 1995), and antimony has been known to substitute for iron or sulphur within pyrite (Qi et al. 2007).

Trace amounts of copper were found within primary pyrite. Remobilised pyrite grains were observed to coexist with chalcopyrite grains, however these chalcopyrite grains were not of sufficient size for quantitative data to be collected.

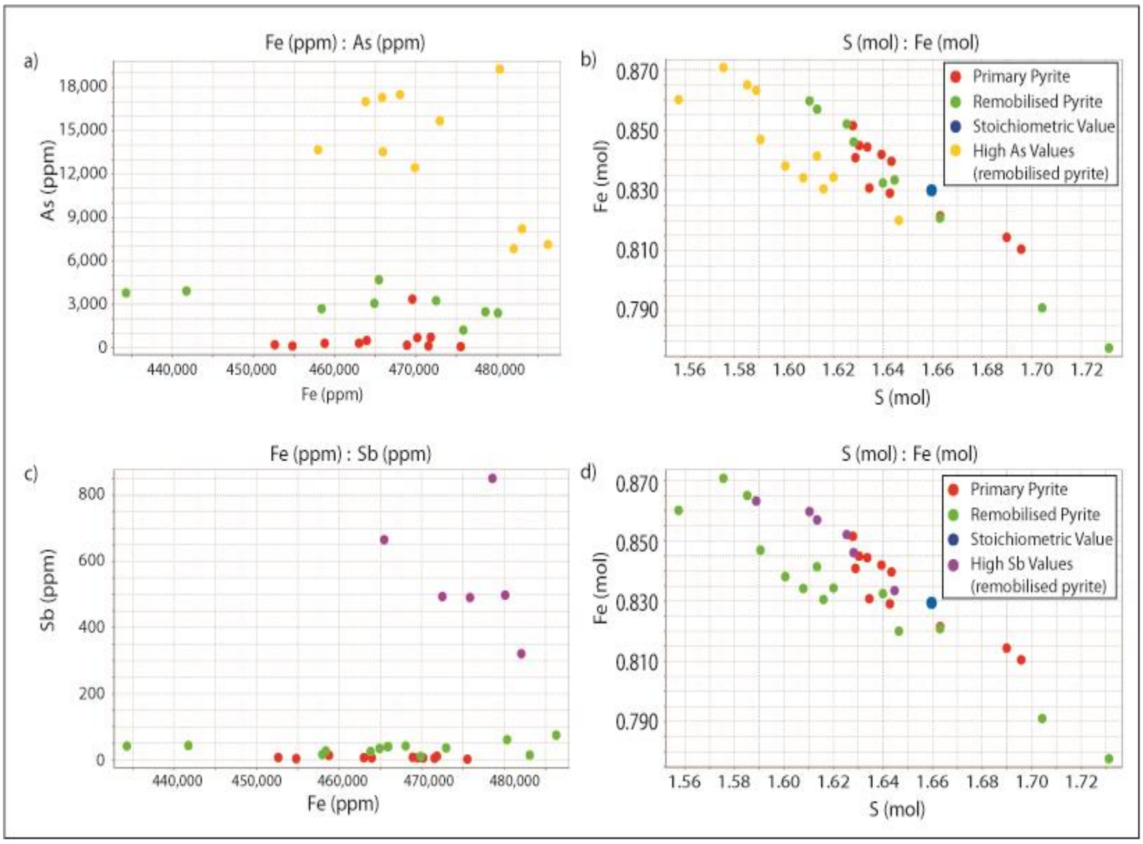

Figure 11: a) Fe (ppm) v. As (ppm) graph highlighting high As values found in remobilised pyrite; b) Fe (mol) v. S (mol) showing high As values in relation to plotted stoichiometric value; c) Fe (ppm) v. Sb (ppm) graph highlighting high Sb values in remobilised pyrite; d) Fe (mol) v. S (mol) showing high Sb values in relation to plotted stoichiometric value.

Cover sequence prospectivity index

Fabris et al. (2013) proposed a prospectivity index towards potential IOCG mineralisation in the central Olympic Domain (Fig. 1) using the elements Ag, As, Bi, Ce, La, Mo, Se, Sb, Te and W. The index is designed to quantitatively estimate the prospectivity of a sample, independent of ore minerals (such as Cu and Au, which do not often have a large footprint associated). Each element with a measured concentration greater than 10x crustal abundance is given a value of 1, and elements with measured concentrations less than 10x crustal abundance are given a value of 0. The prospectivity index is the average of the assigned values for each of the ten elements. A prospectivity index score of >0.8 is highly significant, 0.6 – 0.8 is very significant, and 0.4 – 0.6 is significant (Fabris et al. 2013).

When determining the prospectivity index for the cover lithologies on the Yorke Peninsula, anomalous data from normalised plots (Fig. 10) is excluded when the threshold of 10x average crustal abundance is used. For this reason, 3x crustal average was used to determine samples of interest, as this threshold captures elevated and anomalous data (Fig. 10). Tellurium was excluded as concentrations were below minimum level of detection.

Calculation of the prospectivity index of the samples using the 3x average crustal abundance threshold and consequential mapping shows an area of interest near Bute, in the north-eastern region of the study area (Fig. 12), as well as elevation near Wallaroo, an area of known basement mineralisation.

Use of the cover rocks from drill core across the Yorke Peninsula presents difficulties in interpretation that analysis of the basement rocks does not. Some areas of known basement mineralisation do not show a geochemical anomaly in the cover rocks, illustrating the importance of understanding the relationship between the basement and cover rocks.

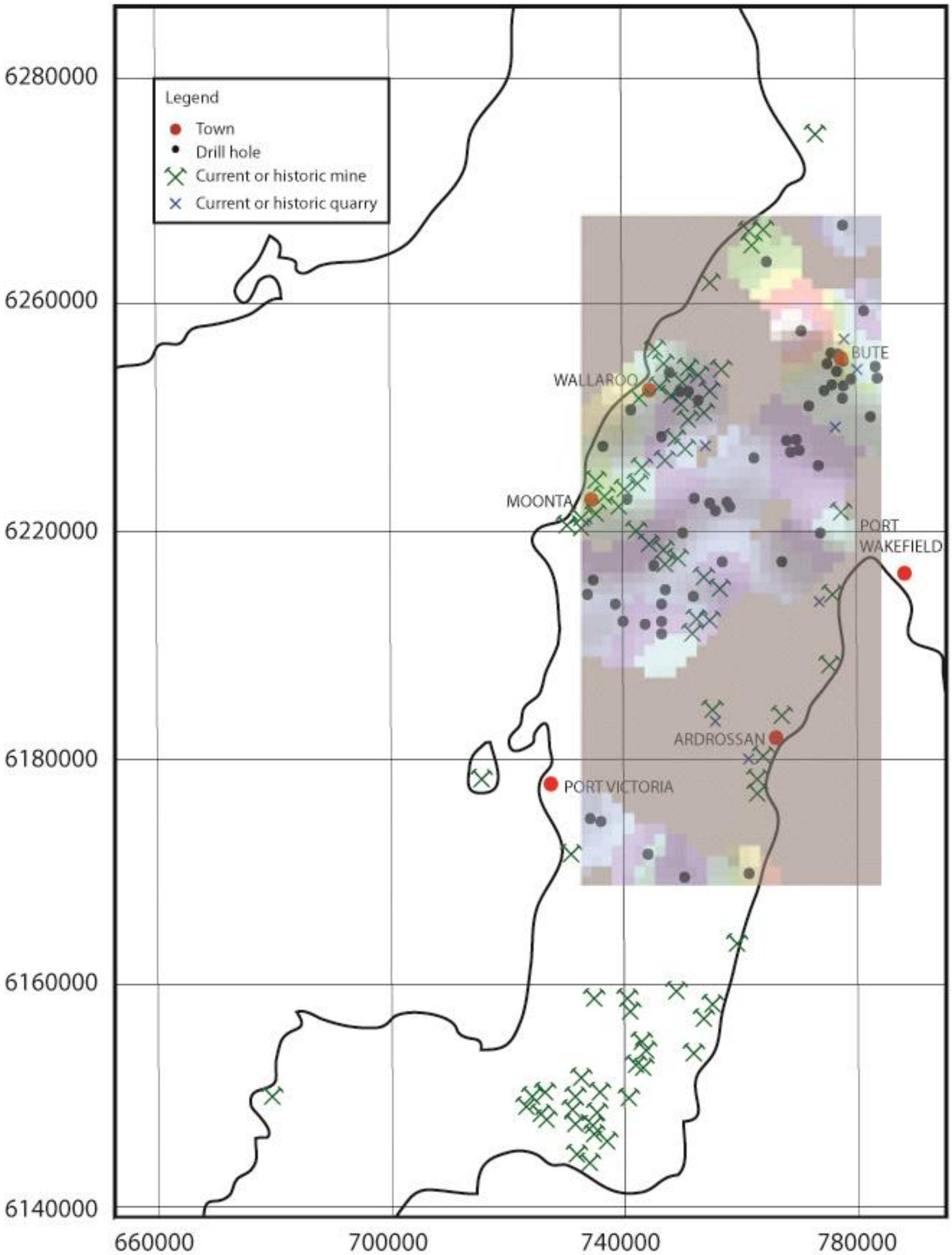

Figure 12: Map of the Yorke Peninsula study area (including drill hole location and current and historic mines and quarries) with gridded cover prospectivity index map overlain, showing potential presentation of basement mineralisation west of Bute and near Wallaroo.

Implications on exploration

As an exploration medium, a 1m composite drill sample of the bottom of cover sequence is an appropriate sample size for characterisation of background geochemistry and identification of pathfinder elements in the cover sequence. Several interesting pathfinder elements (As, Sb) are deployed in pyrite and therefore samples containing pyrite are of importance, as are samples containing other sulphides due to the preference of pathfinder elements to partition into these minerals (Mo in molybdenite, Cu in chalcocite or chalcopyrite, Ag and Bi in bornite) (Cook et al. 2011). Samples containing oxides are also of interest as they are commonly used in IOCG exploration (Mumm et al. 2012, Nadoll et al. 2014).

The prospectivity index proposed by Fabris et al. (2013), initially designed for use on basement samples, appears to be a potential exploration tool for the cover sequence over the Yorke Peninsula once background geochemistry and pathfinder elements have been identified and the threshold is changed to a suitable value. Presentation of a small area of interest over the Wallaroo region (an area of known basement mineralisation) validates this index to a degree, however a larger anomaly over historic and current mine locations is expected, indicating that either cover sequence data directly over mineralisation has not been used (expected as cover sequence samples were likely discarded at the time of mining), or that the dataset utilised is not extensive enough to identify large amounts of lateral dispersion of elements.

An understanding of the depositional and post-depositional environment of the cover sequence is crucial in order to determine the likely transport mechanism of an area of cover sequence. This makes it possible to apply cover sequence data to exploration for basement mineralisation, and allows correction for lateral dispersion of elements away from potential mineralisation (Forbes et al. accepted). Use of diamictite samples require an understanding of palaeotopography and glacial flow directions (Forbes et al. accepted, McClenaghan et al. 2000), while in conglomerate samples remobilisation of pyrite and movement of elements by chemical transport occur, requiring knowledge of past and present phreatic processes (Aspandiar et al. 2008, Britt et al. 2010).

Improvements on experimental design

In order to draw more meaningful conclusions from whole rock geochemical data across an area as large as the Yorke Peninsula, the transport mechanisms of elements from basement mineralisation into the basal cover sequence needs to be investigated at the deposit-scale where known basement mineralisation occurs. Determination of element deployment within samples is needed prior to whole rock geochemical testing, to ensure that minerals hosting pathfinder elements can be identified prior to samples being destroyed. This would allow closer correlation between trace element geochemical data and SEM and LA-ICP-MS data.

A larger sample set is required to accurately determine the whether the modified prospectivity index can be used to target basement mineralisation and to further define potential areas of interest. A greater density of samples across the Yorke Peninsula may give further areas of interest that have not been identified in this study.

Recommendations for further work

While the prospectivity index modified from Fabris et al. (2013) shows areas of potential expression of basement mineralisation in the cover sequence across the Yorke Peninsula at a regional scale, it is recommended that the validity of this index be tested over known basement mineralisation on the Yorke Peninsula, such as the unmined Hillside deposit. This would also test the extent of lateral dispersion as well as zoning of elements at deposit scale. Further work is recommended to determine the deployment of elements that were not found within pyrite in this study, such as Cu, Mo, W and LREEs. Re-evaluation of the modified prospectivity index after validation over known mineralisation with a larger dataset is recommended, to determine whether lateral dispersion of elements can be identified on a regional scale, or whether this index is more suitable for deposit-scale mineralisation.

CONCLUSIONS

The use of the prospectivity index proposed by Fabris et al. (2013) with a 3x average crustal abundance threshold is applicable to the cover sequence in the Yorke Peninsula on a regional scale. Pathfinder elements to basement IOCG mineralisation have been transported into the cover sequence by a combination of mechanical and chemical methods. Pyrite hosts several pathfinder elements (As, Sb, Co, Ni), and should therefore be targeted as a vector towards IOCG mineralisation in the basement rocks, however understanding of depositional and post-depositional environment of the cover sequence is crucial before data can be applied to exploration.

ACKNOWLEDGMENTS

Thanks to Caroline Forbes and David Giles for their advice and comments throughout the project, Rosalind King and Katie Howard for their support throughout the year, Colin Conor for his invaluable knowledge of the study area, Ben Wade and Adelaide Microscopy for analytical advice and instruction, the DET CRC for accesses to reports pertaining to this project, Moonta Core Library for access to drill core, Kym Custance and Aaron Steinert for their advice and discussions throughout the year.

REFERENCES

ANAND R. R. & BUTT C. R. M. 2010 A guide for mineral exploration through the regolith in the Yilgarn Craton, Western Australia, *Australian Journal of Earth Sciences,* vol. 57, pp. 1015-1114.

ANAND R. R.*, et al.* 2001 Regolith evolution and geochemical dispersion in transported and residual regolith - Bronzewing gold deposit, *Geochemistry: Exploration, Environment, Analysis,* vol. 1, pp. 265-276.

ASPANDIAR M. F., ANAND R. R. & GRAY D. J. 2008 Geochemical dispersion mechanisms through transported cover: implications for mineral exploration in Australia. Bentley, Western Australia: CRC LEME.

BRITT A. F., SMITH R. E. & GRAY D. J. 2010 Element mobilities and the Australian regolith - a mineral exploration perspective, *Marine and Freshwater Research,* vol. 52, pp. 25-39.

CHENG Q. 2014 Vertical distribution of elements in regolith over mineral deposits and implications for mapping geochemical weak anomalies in covered areas, *Geochemistry: Exploration, Environment, Analysis,* vol. 14, pp. 277-289.

CONOR C. 1995 Prospectivity re-assessment, and GIS data package: Moonta-Wallaroo region. Mines and Energy South Australia.

CONOR C.*, et al.* 2010 Alteration and mineralisation in the Moonta-Wallaroo Copper-Gold mining field region, Olympic Domain, South Australia. Hydrothermal Iron Oxide Copper-Gold and Related Deposits: A Global Perspective.

CONOR C. H. H. 2002 The Palaeo-Mesoproterozoic geology of northern Yorke Peninsula, South Australia: Hiltaba Suite-related alteration and mineralisation of the Moonta-Wallaroo Cu-Au District.

COOK N. J.*, et al.* 2011 Minor and trace elements in bornite and associated Cu-(Fe)-sulfides: A LA-ICP-MS study, *Geochimica et Cosmochimica Acta,* vol. 75, pp. 6473-6496.

COOK N. J.*, et al.* 2013 Arsenopyrite-pyrite association in an orogenic gold ore: tracing mineralization history from textures and trace elements, *Economic Geology,* vol. 108, no. 1273-1283.

COWLEY W., CONOR C. & ZANG W. 2003 New and revised Proterozoic stratigraphic units on northern Yorke Peninsula, *MESA Journal*, pp. 46-58.

DAILY B. 1990 Cambrian stratigraphy of Yorke Peninsula. In JAGO J. B. & MOORE P. S. eds. The Evolution of a Late Precambrian-Early Palaeozoic rift complex: The Adelaide geosyncline. pp. 215-229. Geological Society of Australia.

FABRIS A., *et al.* 2013 Characterising alteration in the eastern Gawler Craton: regional geochemical trends within an IOCG province. Deep Exploration Technologies CRC.

FISHER L., *et al.* 2013 Links between hypogene expression of mineralisation and lithology at Agnew and regolith response. Deep Exploration Technologies Cooperative Research Centre.

FORBES C. 2012a Report of Sampling Strategy and Background Geochemistry. South Australia: Deep Exploration Technologies CRC.

--- 2012b Update on collection of laboratory whole rock geochemical data. Yorke Peninsula Project. DET CRC.

FORBES C., *et al.* accepted Glacial dispersion of hydrothermal monazite in the Prominent Hill deposit: An exploration tool.

GILES D., HILLIS R. & CLEVERLEY J. 2014 Deep Exploration Technologies Provide the Pathway to Deep Discovery, *SEG Newsletter*, no. 97, pp. 23-27.

GRAVESTOCK D. I. & GATCHOUSE C. G. 1995 Stansbury Basin. In DREXEL J. F. & PREISS W. V. eds. The geology of South Australia Vol 2, The Phanerozoic. pp. 5-19. South Australia: Geological Survey.

GROVES D. I., *et al.* 2010 Iron Oxide Copper-Gold (IOCG) Deposits through Earth History: Implications for Origin, Lithospheric Setting, and Distinction from Other Epigenetic Iron Oxide Deposits, *Economic Geology,* vol. 105, pp. 641-654.

HAND M., REID A. & JAGODZINSKI L. 2007 Tectonic Framework and Evolution of the Gawler Craton, Southern Australia, *Economic Geology,* vol. 102, pp. 1377-1395.

HARVEY S. C. & HIBBURT J. E. 1999 Petroleum exploration and development in South Australia, 12th Edition. Department of Primary Industries and Resources.

HILL E. J., *et al.* 2014 Using geochemical proxies to model nuggety gold deposits: An example from Sunrise Dam, Western Australia, *Journal of Geochemical Exploration,* vol. 145, pp. 12-24.

HOEK J. D. & SCHAEFER B. F. 1998 Palaeoproterozoic Kimban mobile belt, Eyre Peninsula: timing and significance of felsic and mafic magmatism and deformation, *Australian Journal of Earth Sciences,* vol. 45, pp. 305-313.

HUSTON D. L., *et al.* 1995 Trace elements in sulfide minerals from eastern Australian volcanic-hosted massive sulfide deposits, *Economic Geology,* vol. 90, pp. 1167-1196.

JAGO J. B., SUN X. & ZANG W.-L. 2002 Correlation within early Palaeozoic basins of eastern South Australia. Report Book. South Australia: Department of Primary Industries and Resources.

LINTERN M. J. 2014 The association of gold with calcrete, *Ore Geology Reviews,* vol. 66, pp. 132-199.

LINTERN M. J., SHEARD M. J. & CHIVAS A. R. 2006 The source of pedogenic carbonate associated with gold-calcrete anomalies in the western Gawler Craton, South Australia, *Chemical Geology,* vol. 235, pp. 299-324.

MARK G., OLIVER N. H. S. & WILLIAMS P. J. 2006 Mineralogical and chemical evolution of the Ernest Henry Fe oxide-Cu-Au ore system, Cloncurry district, northwest Queensland, Australia, *Mineralium Deposita,* vol. 40, pp. 769-801.
MCCLENAGHAN M. B., THORLEIFSON L. H. & DILABIO R. N. W. 2000 Till geochemical and indicator mineral methods in mineral exploration, *Ore Geology Reviews,* vol. 16, pp. 145-166.
MCQUEEN K. G. 2006 Identifying Geochemical Anomalies. Canberra: CRC LEME.
MCQUEEN K. G., HILL S. M. & FOSTER K. A. 1999 The nature and distribution of regolith carbonate accumulations in southeastern Australia and their potential as a sampling medium in geochemical exploration, *Journal of Geochemical Exploration,* vol. 67, pp. 67-82.
MUMM A. S., DART R. C. & SAY P. 2012 Hematite/maghemite trace element geochemistry in base metal exploration, *Journal of Geochemical Exploration,* vol. 124, pp. 239-251.
NADOLL P.*, et al.* 2014 The chemistry of hydrothermal magnetite: A review, *Ore Geology Reviews,* vol. 61, pp. 1-32.
NISHIYAMA T. 1983 Minor elements in pyrite and chalcopyrite from the Mamut Mine, Malaysia, *Mining Geology,* vol. 33, pp. 1-7.
PRENDERGAST K. 2007 Application of lithogeochemistry to gold exploration in the St Ives goldfield, WA, *Geochemistry: Exploration, Environment, Analysis,* vol. 7, pp. 99-108.
QI C.*, et al.* 2007 Environmental geochemistry of antimony in Chinese coals, *Science of the Total Environment,* vol. 389, pp. 225-234.
RUDNICK R. L. & GAO S. 2004 Composition of the Continental Crust. In RUDNICK R. L. ed. Treatise on geochemistry*.* pp. 1-64. Elsevier.
SCHODDE R. 2014 Uncovering exploration trends and the future: Where's exploration going? International Mining and Resources (IMARC) Conference*.* Melbourne.
SCOTT K. M. & PAIN C. F. 2008 Regolith Science*.* Springer Science + Business Media B.V.
CSIRO Publishing, Dordrecht, The Netherlands
Collingwood, Australia.
SURVEY G. 1995 The geology of South Australia. Vol 2, The Phanerozoic*.* Geological Survey, South Australia.
ZANG W. 2003 Matiland special 1:250 000 geological map, *MESA Journal,* vol. 31, pp. 32-34.

APPENDIX A: DRILL HOLE DETAILS

Samp_R#	DH_No	DH_Name	East	North	Zone	East - original	Depth from	Depth to	Strat_Name	Lith_type	Samp_type
1937385	178246	B 53	776838	6250511	53	776838	20.00	22.00	Kulpura Formation	Calcareous sediment	Cuttings
1949816	23726	Bute B 45	777294	6247803	53	777294	52.70	53.65	Unnamed GIS unit	Calcareous sediment	Drill core
1949801	30064	Bute B40	782811	6239489	54	228478	504.00	505.05	Appila Tillite	Calcareous sediment	Drill core
1937400	22676	SYC 610	750690	6160130	53	750690	96.00	100.00	Winulta Formation	Calcareous sediment	Cuttings
1949785	23723	Bute B 42	777295	6249394	53	777295	69.00	70.00	Unnamed GIS unit	Carbonate	Drill core
1949052	23730	Bute B 50	775944	6248599	53	775944	39.25	40.25	Unnamed GIS unit	Carbonate	Drill core
1949019	30055	Bute B24	778282	6248945	54	223949	100.85	101.85	Unnamed GIS unit	Carbonate	Drill core
1949025	30058	Bute B28	779440	6245971	54	225107	201.20	202.20	Unnamed GIS unit	Carbonate	Drill core
1949010	30059	Bute B29	778561	6248868	54	224228	108.95	109.95	Unnamed GIS unit	Carbonate	Drill core
1949781	23729	Bute B49	776876	6249028	54	222543	88.00	88.20	Unnamed GIS unit	Carbonate	Drill core
1949041	23033	DDH 190	762660	6232342	53	762660	30.60	30.90	Unnamed GIS unit	Carbonate	Drill core
1933084	143968	PJ 1A	761879	6160620	53	761879	208.30	209.30	Stansbury Limestone	Carbonate	Drill core
1947175	23738	AA1	771077	6254479	53	771077	42.00	44.00	Unnamed GIS unit	Clay	Cuttings
1937394	23413	Doora MG 5	746513	6236028	53	746513	6.50	7.16	Unnamed GIS unit	Clay	Drill core
1947187	142667	M 105	747311	6209650	53	747311	8.00	10.00	Unnamed GIS unit	Clay	Cuttings
1937397	143253	M 142	751915	6208687	53	751915	0.00	4.00	Unnamed GIS unit	Clay	Cuttings
1937614	142692	M 169	757073	6214771	53	757073	2.00	4.00	Unnamed GIS unit	Clay	Cuttings
1937616	142693	M 170	757481	6214765	53	757481	10.00	12.00	Unnamed GIS unit	Clay	Cuttings
1947178	143281	M 200	745443	6213456	53	745443	16.00	18.00	Unnamed GIS unit	Clay	Cuttings
1946908	142632	M 23	739599	6204215	53	739599	24.00	26.00	Unnamed GIS unit	Clay	Cuttings
1946910	143205	M 42	743608	6203678	53	743608	10.00	12.00	Unnamed GIS unit	Clay	Cuttings
1947181	142651	M 63	738430	6206920	53	738430	14.00	16.00	Unnamed GIS unit	Clay	Cuttings
1947183	143215	M 64	738441	6207270	53	738441	14.00	16.00	Unnamed GIS unit	Clay	Cuttings
1937403	142663	M 96	751829	6208254	53	751829	10.00	12.00	Unnamed GIS unit	Clay	Cuttings
1933074	23265	Nth Kadina 1	747787	6247265	53	747787	1.50	3.05	Unnamed GIS unit	Clay	Drill core
1933090	22717	Penang Mine DD 2	750382	6219225	53	750382	23.00	24.00	Unnamed GIS unit	Clay	Drill core
1960882	30051	Bute B18	778309	6244444	54	223976	168.80	169.80	Unnamed GIS unit	Conglomerate	Drill core
1949811	23669	DDH 153	751171	6243568	53	751171	115.80	116.74	Winulta Formation	Conglomerate	Drill core

1949803	23672	DDH 156	752805	6242398	53	752805	138.60	139.60	Winulta Formation	Conglomerate	Drill core
1960845	23028	DDH 178	733429	6208620	53	733429	35.30	36.27	Winulta Formation	Conglomerate	Drill core
1949807	23031	DDH 186	755663	6223745	53	755663	81.00	82.00	Winulta Formation	Conglomerate	Drill core
1960885	23037	DDH 194	769374	6233729	53	769374	52.00	53.03	Emeroo Subgroup	Conglomerate	Drill core
1949036	23039	DDH 197	740506	6225440	53	740506	24.60	25.60	Winulta Formation	Conglomerate	Drill core
1949788	23049	DDH 210	769300	6233887	53	769300	81.30	82.30	Emeroo Subgroup	Conglomerate	Drill core
1949793	23701	DDH 212	741389	6240671	53	741389	41.80	42.80	Winulta Formation	Conglomerate	Drill core
1960888	23051	DDH 221	754929	6224206	53	754929	82.50	83.45	Winulta Formation	Conglomerate	Drill core
1949784	23052	DDH 227	752291	6225060	53	752291	112.70	113.70	Winulta Formation	Conglomerate	Drill core
1949039	23054	Bute B 21	774179	6231246	53	774179	405.10	405.20	Sturt Tillite	Diamictite	Drill core
1949796	30047	Bute B14	784258	6246312	54	229925	337.90	338.90	Appila Tillite	Diamictite	Drill core
1949821	30050	Bute B17	781823	6257617	54	227490	291.00	292.00	Appila Tillite	Diamictite	Drill core
1949016	30054	Bute B23	777508	6247943	54	223175	106.30	107.30	Appila Tillite	Diamictite	Drill core
1949022	30056	Bute B25	777364	6250259	54	223031	107.80	108.80	Appila Tillite	Diamictite	Drill core
1937184	29752	Bute DDH7	783721	6248572	54	229388	439.00	440.00	Appila Tillite	Diamictite	Drill core
1949814	23696	DDH 196	768986	6235239	53	768986	181.10	182.12	Unnamed GIS unit	Diamictite	Drill core
0000001		WTDD001	734268	6169901	53	734268	143.10	144.10	Unnamed GIS unit	Diamictite	Drill core
1937388	23748	AA 15	775431	6244530	53	775431	14.00	16.00	Unnamed GIS unit	Sandstone	Cuttings
1949790	23048	DDH 207	770327	6233976	53	770327	40.30	41.30	Emeroo Subgroup	Sandstone	Drill core
1949012	23699	DDH 209	770228	6235144	53	770228	178.90	179.90	Emeroo Subgroup	Sandstone	Drill core
1946897	143186	M 2	746712	6202276	53	746712	16.00	18.00	Unnamed GIS unit	Sandstone	Cuttings
1946899	143188	M 6	746720	6204029	53	746720	18.00	20.00	Unnamed GIS unit	Sandstone	Cuttings
1947185	143230	M 90	746607	6206986	53	746607	2.00	4.00	Unnamed GIS unit	Sandstone	Cuttings
1960848	22962	SYP 602	767704	6214605	53	767704	132.00	134.00	Winulta Formation	Sandstone	Cuttings
1933087	23197	Tickera 2	764842	6266413	53	764842	119.83	120.55	Unnamed GIS unit	Sandstone	Drill core
1960879	30065	Bute B41	778298	6242989	54	223965	157.40	158.35	Unnamed GIS unit	Sandstone/breccia	Drill core
1933072	23389	Bute DDH 6	772223	6241274	53	772223	477.70	478.70	Rhynie Sandstone	Sandstone/breccia	Drill core
1960842	143972	Cur D4	744329	6163730	53	744329	38.50	39.50	Winulta Formation	Sandstone/conglomerate	Drill core
1933077	139489	DD85WE1	734539	6211211	53	734539	32.10	33.10	Winulta Formation	Sandstone/conglomerate	Drill core
1949033	23638	DDH 119	750354	6244057	53	750354	141.00	142.04	Winulta Formation	Sandstone/conglomerate	Drill core
1949031	23021	DDH 149	735724	6234746	53	735724	21.90	22.86	Winulta Formation	Sandstone/conglomerate	Drill core
1949046	23036	DDH 193	758334	6224301	53	758334	24.35	25.35	Winulta Formation	Sandstone/conglomerate	Drill core
1949829	23047	DDH 205	769461	6233877	53	769461	100.50	101.47	Emeroo Subgroup	Sandstone/conglomerate	Drill core
1960890	23697	DDH 206	770244	6235564	53	770244	224.70	225.70	Emeroo Subgroup	Sandstone/conglomerate	Drill core

1960893	23698	DDH 208	769811	6234551	53	769811	270.10	271.10	Emeroo Subgroup	Sandstone/conglomerate	Drill core
1949824	23700	DDH 211	741294	6240971	53	741294	49.60	50.60	Winulta Formation	Sandstone/conglomerate	Drill core
1937382	30263	PB 1	778393	6272671	54	224060	312.00	313.00	Rhynie Sandstone	Sandstone/conglomerate	Drill core
1937179	22963	SYM 600/102	774067	6219496	53	774067	290.40	291.40	Emeroo Group	Sandstone/conglomerate	Drill core
0000004		WTDD003	736061	6169308	53	736061	142.70	143.70	Unnamed GIS unit	Sandstone/conglomerate	Drill core
1949007	30060	Bute B31	777888	6243276	54	223555	136.30	137.30	Unnamed GIS unit	Shale	Drill core
1937391	174055	BRC 1	777406	6244863	54	223073	65.00	68.00	Tapley Hill Formation	Siltstone	Cuttings

APPENDIX B: WHOLE ROCK GEOCHEMISTRY

Table 1a: Whole rock geochemistry for samples 1937385 to 1949807 (inclusive), elements Au - F

Samp_R#	Au (ppb)	Ag (ppm)	Al2O3 (wt%)	As (ppm)	Ba (ppm)	Be (ppm)	Bi (ppm)	CaO (wt%)	Cd (ppm)	Ce (ppm)	Co (ppm)	Cr (ppm)	Cs (ppm)	Cu (ppm)	Dy (ppm)	Er (ppm)	Eu (ppm)	F (ppm)
1937385	0.50	0.40	8.16	247.00	220.70	3.70	1.67	14.11	0.30	68.50	156.80	37.00	4.63	259.00	5.36	2.91	0.99	1213.0
1949816	6.00	0.03	3.43	7.00	104.30	1.20	1.02	23.40	0.10	32.80	20.40	73.00	1.00	63.00	5.26	2.52	1.05	317.00
1949801	6.00	0.03	11.60	42.00	474.50	1.90	2.95	0.65	0.01	66.10	25.40	79.00	3.88	214.00	4.08	2.45	1.11	714.00
1937400	0.50	0.03	7.73	6.00	601.80	1.30	0.04	0.28	0.01	66.70	5.10	29.00	2.85	32.00	5.43	3.14	1.30	425.00
1949785	0.50	0.56	2.59	98.60	144.00	1.20	1.02	24.18	0.07	28.90	43.30	37.00	0.80	46.00	5.91	3.20	0.82	303.00
1949052	0.50	0.28	3.98	28.20	64.80	1.60	0.54	19.15	0.03	75.70	8.50	27.00	0.78	128.00	4.97	2.47	1.24	376.00
1949019	3.00	0.39	0.81	28.20	95.10	0.80	1.54	27.91	0.05	18.10	17.90	36.00	0.29	592.00	2.97	1.51	0.71	177.00
1949025	0.50	0.77	1.83	123.40	74.10	0.80	0.08	24.48	0.08	19.10	63.90	37.00	0.88	57.00	1.71	0.80	0.39	307.00
1949010	0.50	0.69	1.02	33.70	87.00	0.50	0.17	26.43	0.06	15.10	19.00	38.00	0.26	602.00	2.24	1.10	0.52	222.00
1949781	0.50	0.71	1.21	94.20	87.00	0.80	0.11	27.30	0.06	28.80	41.30	37.00	0.52	258.00	5.80	2.90	1.23	216.00
1949041	0.50	0.03	3.24	5.60	166.30	1.20	0.01	20.51	0.03	56.50	4.70	37.00	0.48	60.00	3.68	1.98	0.83	300.00
1933084	0.50	0.92	4.40	32.00	141.50	0.25	0.07	37.80	0.01	23.40	11.40	10.00	0.85	303.00	1.73	0.99	0.41	176.00
1947175	27.00	0.49	18.02	61.50	210.50	3.70	0.45	0.06	0.02	212.40	69.40	111.00	8.63	98.00	10.03	5.32	2.10	987.00
1937394	0.50	0.10	7.85	6.10	805.00	1.40	0.09	0.07	0.46	69.40	5.50	10.00	3.66	52.00	5.44	4.05	0.72	420.00
1947187	0.50	0.08	8.95	10.80	180.60	1.60	0.03	0.58	0.01	53.30	1.50	169.00	0.86	0.50	5.15	3.19	0.77	180.00
1937397	0.50	0.03	8.78	10.90	339.50	1.00	0.13	8.83	0.01	37.00	6.00	41.00	2.59	16.00	3.08	1.80	0.73	337.00
1937614	0.50	0.03	9.70	15.00	235.80	0.90	0.13	6.58	0.04	31.90	7.20	109.00	2.71	16.00	2.51	1.44	0.62	425.00
1937616	0.50	0.07	15.02	3.40	82.60	3.10	0.04	1.61	0.01	46.60	19.10	35.00	1.64	83.00	5.07	2.94	1.27	573.00
1947178	0.50	0.12	23.86	12.30	489.60	3.60	0.01	0.02	0.01	6.40	4.10	176.00	7.12	64.00	1.85	1.65	0.28	1222.0
1946908	0.50	0.06	19.27	4.50	1359.40	2.50	0.02	4.80	0.01	184.90	25.00	140.00	1.48	110.00	15.95	9.58	4.11	1039.0
1946910	0.50	0.03	16.38	4.50	2221.60	1.70	0.03	0.41	0.01	58.80	1.10	97.00	2.03	4.00	1.26	0.83	0.52	286.00
1947181	0.50	0.23	13.34	5.20	476.60	0.90	0.29	3.16	0.02	23.90	5.20	117.00	4.29	18.00	1.97	1.36	0.43	418.00
1947183	0.50	0.03	20.90	0.50	199.30	2.00	0.03	2.31	0.01	22.40	14.00	189.00	2.48	20.00	0.90	0.61	0.26	1383.0
1937403	0.50	0.03	11.41	1.70	372.60	2.10	0.08	0.69	0.01	7.70	4.20	49.00	2.70	10.00	1.55	1.25	0.22	554.00
1933074	0.50	0.03	9.32	23.80	1080.90	0.90	0.22	0.35	7.09	25.50	3.20	54.00	3.76	40.00	1.96	1.31	0.39	1331.0
1933090	0.50	0.03	14.79	3.00	1396.90	3.80	0.07	0.06	0.13	72.50	10.70	10.00	4.90	98.00	4.71	3.45	0.74	495.00
1960882	2.00	0.90	8.48	318.00	1626.70	2.30	0.24	8.80	0.01	42.10	118.80	39.00	3.24	145.00	3.02	1.72	0.62	826.00
1949811	0.50	0.03	6.33	4.00	273.60	1.40	0.11	10.59	0.01	53.30	10.40	41.00	1.10	32.00	5.01	2.67	1.44	839.00
1949803	0.50	0.03	3.09	4.00	167.90	0.60	0.03	0.15	0.01	32.60	1.20	10.00	0.69	498.00	1.17	0.69	0.52	136.00
1960845	0.50	0.03	5.60	5.00	218.20	1.40	0.05	0.07	0.01	71.30	8.40	21.00	0.80	19.00	4.57	2.88	0.63	561.00
1949807	0.50	0.03	2.51	4.00	161.70	0.25	0.01	4.42	0.01	81.40	2.00	10.00	0.62	16.00	6.41	3.61	1.43	292.00

Table 1b: Whole rock geochemistry for samples 1937385 to 1949807 (inclusive), elements Fe_2O_3 - Ni

Samp_R#	Fe2O3 (wt%)	Ga (ppm)	Gd (ppm)	Ge (ppm)	Hf (ppm)	Ho (ppm)	In (ppm)	K2O (wt%)	La (ppm)	Li (ppm)	Lu (ppm)	MgO (wt%)	MnO (wt%)	Mo (ppm)	Na2O (wt%)	Nb (ppm)	Nd (ppm)	Ni (ppm)
1937385	5.51	12.00	5.25	1.20	3.20	1.04	0.05	4.27	43.40	20.00	0.42	10.57	0.40	5.20	0.19	9.90	26.80	52.00
1949816	4.82	8.10	5.35	0.30	1.10	1.00	0.05	1.05	15.20	13.30	0.31	15.94	0.91	4.90	0.69	3.30	17.20	47.00
1949801	7.89	15.30	4.70	0.80	6.20	0.83	0.04	3.53	32.00	54.30	0.38	2.77	0.05	1.30	1.14	12.18	28.30	47.00
1937400	4.76	10.90	5.62	0.99	7.00	1.10	0.03	4.91	34.30	8.60	0.50	0.63	0.02	1.80	0.51	16.80	28.60	10.00
1949785	4.73	5.10	4.75	0.15	1.00	1.19	0.12	1.20	14.80	5.80	0.37	15.44	1.01	2.00	0.24	5.95	11.80	17.00
1949052	3.45	6.50	5.95	0.03	1.60	0.93	0.07	0.74	35.20	5.10	0.30	13.05	0.62	2.20	1.11	6.74	32.80	5.00
1949019	3.70	2.10	3.16	0.03	0.40	0.58	0.12	0.55	8.10	1.80	0.17	16.73	0.99	3.90	0.05	1.31	8.40	3.00
1949025	3.12	2.80	1.94	0.12	0.90	0.31	0.04	0.96	13.00	5.90	0.11	15.55	0.71	6.20	0.07	3.10	7.80	14.00
1949010	4.12	2.30	2.35	0.03	0.50	0.43	0.08	0.66	7.80	1.40	0.12	17.73	0.98	2.00	0.08	1.54	6.70	7.00
1949781	5.93	3.60	5.19	0.06	0.80	1.12	0.19	0.66	15.10	3.80	1.00	16.45	1.21	1.40	0.12	2.27	13.90	26.00
1949041	4.92	5.10	4.56	0.12	1.10	0.73	0.04	0.23	30.70	6.80	0.25	14.08	1.10	0.50	1.27	1.35	24.40	1.00
1933084	1.09	5.70	2.06	0.85	2.10	0.35	0.01	1.33	12.00	1.40	0.16	0.87	0.11	4.50	1.59	2.10	10.70	2.00
1947175	1.50	29.00	11.39	2.11	9.60	2.02	0.27	2.02	129.10	43.90	0.80	0.70	0.29	5.10	0.29	54.90	83.00	52.00
1937394	9.94	20.40	4.16	1.23	9.90	1.28	0.02	3.98	34.30	7.80	0.77	0.38	0.01	1.90	0.34	30.30	24.50	2.00
1947187	3.51	13.00	4.30	0.91	6.70	1.16	0.02	0.35	54.20	5.20	0.49	0.17	0.01	1.60	4.06	19.50	22.50	0.05
1937397	4.74	12.40	3.01	1.42	4.60	0.61	0.04	1.19	19.10	17.00	0.30	1.49	0.01	0.90	0.91	6.10	17.00	12.00
1937614	4.11	11.60	2.65	0.10	3.60	0.56	0.04	1.21	16.60	21.60	0.22	1.97	0.01	1.30	0.71	6.40	14.50	12.00
1937616	12.75	23.50	4.88	1.39	5.20	1.02	0.19	0.58	27.60	2.40	0.46	0.64	0.01	0.90	4.04	16.70	20.20	13.00
1947178	2.87	37.40	0.78	1.77	4.10	0.48	0.05	5.49	3.30	26.70	0.28	1.17	0.01	2.30	0.36	19.80	2.40	11.00
1946908	9.63	23.30	15.34	1.01	3.00	3.48	0.07	1.62	85.30	17.20	1.28	1.53	0.04	0.50	3.73	7.10	84.90	64.00
1946910	3.23	22.10	1.38	0.73	10.70	0.28	0.04	4.89	44.30	2.60	0.15	0.12	0.01	0.40	3.82	16.80	16.20	1.00
1947181	5.55	17.90	1.70	0.47	6.30	0.45	0.05	1.71	15.10	14.80	0.26	1.07	0.02	1.00	0.92	12.30	9.80	10.00
1947183	9.07	17.30	0.84	0.56	1.10	0.20	0.11	1.71	9.60	15.30	0.08	1.82	0.01	0.40	3.83	3.50	4.30	39.00
1937403	5.53	16.30	0.82	0.65	4.60	0.37	0.04	2.23	4.10	6.50	0.26	0.56	0.01	0.60	3.16	7.20	3.40	7.00
1933074	6.05	17.40	1.59	0.81	7.70	0.42	0.04	2.02	14.90	18.50	0.27	1.24	0.01	2.60	1.20	10.50	10.10	7.00
1933090	7.65	19.70	3.34	1.70	7.10	1.11	0.04	8.18	14.80	11.10	0.54	0.31	0.01	2.10	0.67	16.60	12.50	7.00
1960882	3.69	12.00	3.18	0.80	4.10	0.61	0.06	3.46	21.30	25.60	0.28	6.51	0.40	3.10	0.61	7.86	17.60	59.00
1949811	5.15	9.50	5.81	0.70	9.80	0.97	0.08	2.59	30.20	24.10	0.44	5.12	0.16	0.40	0.37	5.70	25.20	33.00
1949803	2.03	3.10	1.72	0.40	3.10	0.22	0.00	1.89	16.20	12.80	0.16	0.18	0.01	0.40	0.28	2.43	11.90	5.00
1960845	5.97	8.90	4.67	0.80	7.40	0.99	0.01	2.03	36.20	20.50	0.47	0.96	0.03	0.90	0.93	10.55	30.20	35.00
1949807	2.52	3.00	6.67	0.70	1.60	1.32	0.04	1.42	35.60	14.40	0.54	0.88	0.07	0.50	0.05	2.31	35.10	14.00

Table 1c: Whole rock geochemistry for samples 1937385 to 1949807 (inclusive), elements P_2O_5 - Th

Samp_R#	P2O5 (wt%)	Pb (ppm)	Pd (ppm)	Pr (ppm)	Pt (ppb)	Rb (ppm)	Re (ppm)	S (ppm)	Sb (ppm)	Sc (ppm)	Se (ppm)	SiO2 (wt%)	Sm (ppm)	Sn (ppm)	Sr (ppm)	Ta (ppm)	Tb (ppm)	Te (ppm)	Th (ppm)
1937385	0.15	117.00	0.05	7.33	0.05	151.10	0.00	172.00	2.29	12.00	0.03	32.07	5.39	4.00	94.00	1.20	0.80	0.05	14.34
1949816	0.04	10.00	0.05	4.07	1.00	39.70	0.00	437.00	0.43	1.00	0.03	14.21	4.43	1.00	70.50	0.50	0.85	0.05	3.70
1949801	0.14	10.00	0.05	7.53	0.05	151.10	0.00	1078.00	1.40	12.00	0.03	69.37	5.62	3.00	34.40	1.50	0.65	0.10	14.62
1937400	0.21	10.00	0.05	7.27	0.05	176.00	0.00	25.00	0.16	10.00	3.60	80.31	5.81	4.00	44.80	1.60	0.82	0.22	12.81
1949785	0.09	10.00	0.05	2.89	0.05	42.30	0.01	7527.00	0.73	10.00	3.30	13.39	3.44	0.05	68.50	0.30	0.90	0.05	3.87
1949052	0.07	2.50	0.05	8.49	0.05	35.70	0.00	25.00	0.23	10.00	1.40	29.87	6.99	0.05	74.50	0.60	0.83	0.05	9.07
1949019	0.05	2.50	0.05	1.97	0.05	17.50	0.00	3983.00	0.71	14.00	6.60	4.45	2.51	0.05	69.80	0.10	0.50	0.05	1.97
1949025	0.05	391.00	0.05	2.05	0.05	33.90	0.00	5224.00	1.79	10.00	2.40	12.97	1.93	0.05	73.60	0.30	0.28	0.05	3.54
1949010	0.01	10.00	0.05	1.63	0.05	20.90	0.01	6551.00	0.94	10.00	1.50	5.26	1.85	0.05	67.60	0.10	0.37	0.05	2.00
1949781	0.05	11.00	0.05	3.32	0.05	24.90	0.00	12973.00	1.08	22.00	4.10	6.12	4.25	0.05	72.70	0.20	0.91	0.05	2.70
1949041	0.13	2.50	0.05	6.60	3.00	11.80	0.00	25.00	0.08	10.00	4.50	22.89	4.76	1.00	43.80	0.30	0.61	0.05	3.93
1933084	0.04	8.00	0.05	2.78	0.05	48.30	0.01	4312.00	1.23	10.00	4.00	23.22	2.24	2.00	125.10	0.60	0.28	0.20	4.49
1947175	0.09	141.00	0.05	24.11	0.05	165.40	0.03	220.00	1.80	20.00	2.00	68.73	14.78	9.00	30.40	4.80	1.63	0.06	60.39
1937394	0.02	6.00	0.05	6.84	0.05	240.30	0.01	230.00	0.64	10.00	6.10	72.46	4.34	6.00	36.30	2.20	0.72	0.10	20.71
1947187	0.02	9.00	0.05	6.50	0.05	19.50	0.01	75.00	1.69	10.00	4.50	77.39	4.23	4.00	55.70	1.50	0.74	0.05	15.87
1937397	0.06	11.00	0.05	4.29	0.05	54.70	0.00	339.00	0.33	10.00	2.60	57.82	3.46	2.00	315.00	0.90	0.45	0.22	10.92
1937614	0.02	12.00	0.05	3.83	0.05	51.60	0.01	489.00	0.40	10.00	3.00	56.97	2.89	2.00	250.90	0.50	0.39	0.05	7.85
1937616	0.08	8.00	2.00	5.40	1.00	25.50	0.00	295.00	0.15	41.00	1.00	56.03	4.75	4.00	170.30	1.30	0.78	0.05	12.24
1947178	0.02	2.50	0.05	0.65	0.05	298.80	0.00	219.00	0.20	24.00	0.80	55.98	0.53	9.00	15.10	1.70	0.20	0.05	25.39
1946908	0.42	29.00	0.05	20.92	0.05	65.20	0.01	785.00	0.10	25.00	0.90	52.42	16.08	2.00	1220.10	0.60	2.29	0.05	12.48
1946910	0.05	15.00	0.05	5.35	0.05	136.40	0.00	265.00	0.16	10.00	3.80	66.43	2.33	3.00	191.50	1.00	0.18	0.05	10.07
1947181	0.02	13.00	0.05	2.68	0.05	76.80	0.00	633.00	0.44	12.00	2.60	60.38	1.85	4.00	130.00	1.00	0.26	0.06	10.87
1947183	0.02	11.00	6.00	1.17	7.00	185.10	0.00	332.00	0.03	32.00	2.70	49.84	0.84	2.00	168.10	0.20	0.12	0.05	1.71
1937403	0.04	6.00	0.05	0.88	0.05	123.10	0.00	187.00	0.31	10.00	3.60	71.48	0.76	3.00	99.10	0.90	0.19	0.05	7.74
1933074	0.10	18.00	1.00	2.76	0.05	99.70	0.00	540.00	1.13	10.00	4.00	70.33	2.00	6.00	171.10	1.30	0.28	0.10	12.16
1933090	0.10	2.50	0.05	3.27	0.05	555.60	0.00	364.00	0.29	10.00	0.03	63.78	2.72	15.00	57.00	3.90	0.57	0.05	15.94
1960882	0.13	64.00	0.05	4.66	2.00	142.80	0.00	9657.00	3.29	1.00	0.03	53.35	3.39	3.00	23.00	1.00	0.47	0.05	10.75
1949811	0.20	8.00	0.05	6.49	0.05	86.80	0.00	210.00	0.29	1.00	0.03	57.58	5.80	3.00	67.20	1.00	0.80	0.05	12.13
1949803	0.01	2.50	0.05	3.33	0.05	63.90	0.00	593.00	0.23	1.00	0.03	92.60	2.20	2.00	9.50	0.80	0.21	0.05	4.88
1960845	0.07	2.50	0.05	7.81	2.00	61.50	0.00	104.00	0.33	1.00	0.03	83.61	5.73	3.00	27.90	1.20	0.68	0.05	11.64
1949807	0.04	2.50	0.05	9.22	0.05	48.20	0.00	312.00	0.17	1.00	0.03	84.58	7.33	2.00	25.90	0.40	1.00	0.05	5.64

Table 1d: Whole rock geochemistry for samples 1937385 to 1949807 (inclusive), elements TiO_2 - Zr

Samp_R#	TiO2 (wt%)	Tl (ppm)	Tm (ppm)	U (ppm)	V (ppm)	W (ppm)	Y (ppm)	Yb (ppm)	Zn (ppm)	Zr (ppm)
1937385	0.53	2.00	0.43	2.74	102.00	1.00	30.10	2.54	34.00	122.00
1949816	0.30	0.57	0.35	2.36	56.00	4.00	28.90	2.03	94.00	41.00
1949801	0.72	0.58	0.38	2.78	99.00	4.00	22.90	2.43	72.00	214.00
1937400	0.39	0.81	0.57	1.65	31.00	3.00	31.20	2.88	29.00	271.00
1949785	0.17	2.11	0.43	1.80	34.00	1.00	27.20	2.50	39.00	39.00
1949052	0.16	0.38	0.36	2.04	29.00	1.00	24.10	2.08	27.00	59.00
1949019	0.07	0.85	0.21	5.30	34.00	0.05	17.50	1.18	44.00	17.00
1949025	0.17	0.65	0.11	1.99	22.00	0.05	9.40	0.68	19.00	37.00
1949010	0.08	1.83	0.14	2.35	16.00	0.05	13.00	0.84	33.00	19.00
1949781	0.12	12.93	0.40	2.09	43.00	0.05	27.30	2.26	37.00	31.00
1949041	0.16	0.06	0.27	1.80	19.00	2.00	23.90	1.66	63.00	39.00
1933084	0.15	0.27	0.20	5.86	26.00	0.05	12.20	0.92	35.00	74.00
1947175	1.43	2.16	0.84	7.21	141.00	4.00	53.50	5.41	132.00	344.00
1937394	0.44	0.51	0.66	3.56	31.00	3.00	39.70	4.74	16.00	356.00
1947187	0.25	0.06	0.51	2.22	61.00	3.00	33.80	3.36	4.00	271.00
1937397	0.41	0.27	0.29	1.68	69.00	1.00	17.50	1.71	29.00	160.00
1937614	0.40	0.30	0.23	2.04	105.00	2.00	14.40	1.43	41.00	138.00
1937616	2.27	0.06	0.45	6.79	400.00	1.00	20.00	2.94	27.00	190.00
1947178	0.85	0.60	0.25	3.76	138.00	2.00	15.00	1.86	23.00	149.00
1946908	1.03	0.16	1.43	3.65	237.00	0.05	101.90	8.53	77.00	98.00
1946910	0.58	0.44	0.13	2.14	37.00	0.05	7.10	0.98	21.00	445.00
1947181	0.75	0.37	0.20	1.69	104.00	2.00	12.20	1.46	39.00	236.00
1947183	0.47	0.25	0.09	1.18	192.00	0.05	5.90	0.58	27.00	53.00
1937403	0.42	0.63	0.25	3.00	72.00	1.00	9.80	1.48	17.00	173.00
1933074	0.70	0.40	0.27	4.84	277.00	34.00	12.10	1.52	55.00	287.00
1933090	0.39	1.10	0.53	6.19	24.00	14.00	30.60	3.33	56.00	267.00
1960882	0.40	1.27	0.21	2.60	51.00	5.00	17.90	1.73	13.00	148.00
1949811	0.32	0.27	0.41	3.23	44.00	2.00	29.70	2.63	51.00	359.00
1949803	0.11	0.18	0.10	1.11	13.00	2.00	6.70	0.65	0.05	120.00
1960845	0.31	0.19	0.41	5.72	36.00	1.00	29.30	2.92	71.00	267.00
1949807	0.07	0.18	0.55	1.66	5.00	0.05	36.30	3.56	47.00	53.00

Table 2a: Whole rock geochemistry for samples 1937885 to 1937391 (inclusive), elements Au - F

Samp_R#	Au (ppb)	Ag (ppm)	Al2O3 (wt%)	As (ppm)	Ba (ppm)	Be (ppm)	Bi (ppm)	CaO (wt%)	Cd (ppm)	Ce (ppm)	Co (ppm)	Cr (ppm)	Cs (ppm)	Cu (ppm)	Dy (ppm)	Er (ppm)	Eu (ppm)	F (ppm)
1960885	15.00	0.03	12.38	2.00	507.40	3.90	0.25	0.45	0.01	96.00	13.30	107.00	11.68	29.00	4.48	2.49	1.12	1684.0
1949036	2.00	0.03	8.87	15.90	220.50	1.30	0.02	0.03	0.02	489.50	5.10	10.00	0.50	155.00	14.93	7.57	5.70	938.00
1949788	18.00	0.09	9.27	13.30	434.80	2.40	1.01	0.42	0.01	120.40	9.40	84.00	5.30	11.00	11.85	5.68	1.72	915.00
1949793	0.50	0.17	10.47	19.00	619.50	1.20	0.08	0.33	0.01	197.90	7.50	34.00	1.42	132.00	4.99	3.27	2.32	942.00
1960888	0.50	0.03	2.30	3.00	173.00	0.25	0.01	0.07	0.01	59.30	1.10	10.00	0.75	9.00	2.22	1.26	0.60	133.00
1949784	0.50	0.33	4.11	9.40	366.30	0.25	0.16	0.26	0.01	27.70	1.90	10.00	0.99	32.00	6.56	4.30	0.48	132.00
1949039	2.00	0.07	13.78	22.60	506.60	3.30	0.38	0.98	0.03	102.00	16.50	65.00	10.77	61.00	6.09	3.62	1.53	1160.0
1949796	1.00	0.19	13.44	196.80	605.00	3.70	10.54	0.74	0.05	82.60	30.70	80.00	4.93	114.00	4.65	2.89	1.15	864.00
1949821	1.00	0.03	13.09	8.00	615.00	4.00	0.11	4.61	0.10	99.40	10.00	69.00	6.33	67.00	5.94	3.45	1.51	1363.0
1949016	2.00	1.08	12.08	79.00	577.60	5.00	0.90	3.50	0.03	61.10	57.70	79.00	5.18	316.00	4.52	2.66	0.99	1241.0
1949022	1.00	0.48	12.01	22.10	587.50	4.70	5.08	4.03	0.05	63.90	18.60	72.00	4.85	571.00	5.55	3.34	1.08	1254.0
1937184	5.00	0.03	12.34	4.00	538.10	1.30	0.24	1.60	0.08	100.90	21.80	45.00	1.61	35.00	6.08	4.02	1.43	684.00
1949814	235.00	0.03	6.83	3.00	328.70	1.70	0.01	0.58	0.01	72.40	6.90	42.00	3.85	19.00	3.51	2.06	0.95	671.00
0000001	0.50	0.03	15.43	5.00	576.70	2.10	0.04	2.55	0.20	87.50	23.00	77.00	6.09	33.00	5.60	3.03	1.29	753.00
1937388	0.50	0.03	7.38	15.30	244.00	0.90	0.15	0.09	0.01	31.50	1.40	45.00	4.60	16.00	3.79	2.22	0.65	259.00
1949790	0.50	0.06	6.57	23.50	295.50	1.60	0.07	0.04	0.03	73.20	3.60	10.00	9.03	76.00	3.42	1.73	1.15	555.00
1949012	2.00	0.12	6.48	7.10	290.00	0.60	0.06	0.47	0.01	70.60	5.00	28.00	2.29	11.00	4.63	2.62	1.41	364.00
1946897	0.50	0.13	15.02	1.20	579.90	3.30	0.10	0.63	0.01	1036.10	8.50	135.00	4.09	56.00	58.27	25.76	15.64	846.00
1946899	0.50	0.03	17.24	5.10	790.40	3.10	0.03	0.12	0.01	81.60	9.30	152.00	12.81	16.00	4.16	2.37	1.03	1384.0
1947185	0.50	0.03	13.96	3.20	418.50	1.70	0.14	1.75	0.01	74.50	4.50	131.00	2.50	8.00	4.52	2.22	1.09	377.00
1960848	0.50	0.03	4.17	6.00	239.60	1.00	0.01	0.96	0.01	129.20	11.30	10.00	0.77	63.00	8.07	4.09	1.18	339.00
1933087	0.50	0.20	11.98	3.40	280.40	6.10	0.03	0.10	0.01	235.50	4.70	10.00	7.16	27.00	14.50	9.20	1.43	1076.0
1960879	4.00	0.50	2.52	51.00	242.00	1.20	1.71	23.10	0.01	34.70	23.50	25.00	1.33	63.00	2.23	1.09	0.64	346.00
1933072	0.50	0.03	12.75	8.50	802.40	4.20	0.24	4.64	0.08	185.50	9.70	57.00	8.64	18.00	9.56	4.47	2.63	1294.0
1960842	2.00	0.50	5.31	105.00	384.60	1.20	0.05	16.67	0.20	45.20	28.20	46.00	1.17	156.00	5.75	3.72	0.88	340.00
1933077	0.50	0.03	6.69	4.30	333.40	1.20	0.03	0.18	0.01	17.10	3.10	26.00	1.75	10.00	3.64	2.41	0.48	434.00
1949033	5.00	0.17	9.05	22.90	561.80	4.40	0.11	0.30	0.04	46.60	8.80	48.00	7.59	34.00	3.47	1.86	0.95	1055.0
1949031	0.50	0.03	6.20	19.40	140.50	1.30	0.11	2.49	0.03	546.20	5.20	33.00	0.30	16.00	60.68	32.56	7.60	528.00
1949046	0.50	0.03	4.05	8.00	233.20	0.60	0.05	0.10	0.01	49.70	6.10	23.00	1.37	14.00	2.65	1.69	0.57	232.00
1949829	18.00	0.03	9.99	4.00	432.40	3.50	0.07	0.58	0.01	95.70	19.10	38.00	14.05	45.00	4.16	2.42	1.21	1176.0
1960890	1.00	0.03	4.90	6.00	238.20	0.90	0.09	0.50	0.01	40.30	3.10	21.00	4.02	10.00	2.00	1.13	0.63	410.00
1960893	9.00	0.03	7.14	4.00	329.40	1.50	0.04	1.49	0.01	78.50	4.30	35.00	4.08	20.00	3.69	1.91	1.09	594.00
1949824	0.50	0.03	8.96	4.00	285.60	2.20	0.09	0.26	0.01	53.30	14.20	45.00	2.49	44.00	3.15	1.74	0.93	1055.0
1937382	0.50	0.03	6.96	3.70	542.60	0.80	0.05	0.29	0.01	81.00	5.00	27.00	2.47	5.00	2.87	1.67	0.79	509.00
1937179	0.50	0.03	9.59	6.00	366.10	1.20	0.51	0.45	0.01	61.80	19.50	74.00	6.20	10.00	3.53	2.11	0.99	482.00
0000004	0.50	0.03	5.09	0.50	152.50	1.50	0.05	20.09	0.01	54.50	8.50	54.00	1.41	35.00	3.79	2.24	0.77	470.00
1949007	0.50	1.02	1.68	157.70	92.90	1.10	0.37	23.27	0.04	22.10	66.20	42.00	1.04	41.00	1.95	1.09	0.53	259.00
1937391	1.00	0.20	5.66	12.80	203.20	2.50	0.21	18.90	0.31	38.20	4.30	24.00	3.85	30.00	3.27	1.75	0.82	942.00

Table 2b: Whole rock geochemistry for samples 1937885 to 1937391 (inclusive), elements Fe_2O_3 - Ni

Samp_R#	Fe2O3 (wt%)	Ga (ppm)	Gd (ppm)	Ge (ppm)	Hf (ppm)	Ho (ppm)	In (ppm)	K2O (wt%)	La (ppm)	Li (ppm)	Lu (ppm)	MgO (wt%)	MnO (wt%)	Mo (ppm)	Na2O (wt%)	Nb (ppm)	Nd (ppm)	Ni (ppm)
1960885	6.23	18.60	5.50	1.30	3.60	0.89	0.05	5.12	52.60	40.30	0.37	2.55	0.05	0.40	0.09	11.23	38.50	43.00
1949036	3.33	9.00	23.91	0.52	6.30	2.88	0.03	3.01	231.50	20.70	1.02	1.29	0.01	0.10	0.22	10.55	208.70	9.00
1949788	7.81	13.10	10.74	0.66	3.70	2.30	0.03	3.95	62.50	29.40	0.59	1.70	0.07	0.40	0.10	9.83	48.10	14.00
1949793	8.01	15.40	8.76	0.51	8.70	1.05	0.02	5.83	99.00	35.50	0.68	2.46	0.03	0.50	0.65	11.82	78.30	15.00
1960888	2.06	2.30	2.63	0.70	2.90	0.43	0.00	1.72	24.90	8.10	0.20	0.10	0.01	0.40	0.04	2.82	22.00	5.00
1949784	2.33	3.70	2.98	0.72	1.80	1.53	0.01	3.10	13.30	4.30	0.49	0.18	0.03	0.80	0.11	3.47	8.70	0.05
1949039	5.74	19.50	6.76	0.54	6.10	1.26	0.09	4.28	52.00	69.70	0.52	3.24	0.04	1.10	1.56	15.19	41.70	25.00
1949796	6.00	18.40	5.40	0.54	5.90	0.99	0.07	4.65	42.10	66.50	0.45	3.78	0.03	0.80	1.05	14.98	35.00	28.00
1949821	5.45	19.60	6.29	1.20	13.40	1.22	0.06	4.48	52.70	47.30	0.51	4.56	0.30	0.60	1.13	12.88	39.40	47.00
1949016	4.13	17.20	4.60	0.37	5.80	0.93	0.07	4.85	29.60	49.10	0.45	3.55	0.18	1.90	1.65	12.66	26.40	35.00
1949022	5.15	17.90	5.56	0.63	5.80	1.12	0.09	4.36	33.50	36.90	0.51	3.90	0.24	1.30	1.20	13.25	26.20	19.00
1937184	7.75	17.60	5.94	1.38	7.90	1.35	0.03	3.11	52.40	73.70	0.66	4.88	0.04	1.70	1.71	19.80	43.70	48.00
1949814	3.01	8.50	3.95	0.60	3.60	0.74	0.02	4.05	42.20	18.60	0.45	0.97	0.01	0.30	0.10	4.58	27.10	18.00
0000001	9.30	22.80	6.08	0.60	4.90	1.10	0.06	3.03	43.60	29.20	0.50	3.07	0.13	0.30	4.42	13.67	36.50	47.00
1937388	1.89	12.50	2.99	1.95	8.10	0.78	0.03	1.09	19.30	17.00	0.36	0.44	0.01	2.00	0.12	13.80	14.40	6.00
1949790	3.59	6.60	4.29	0.53	2.70	0.65	0.13	3.58	39.00	10.70	0.24	0.36	0.01	0.80	0.12	2.87	32.10	4.00
1949012	3.47	7.20	4.97	0.60	3.20	0.97	0.02	4.03	38.20	19.40	0.35	1.28	0.03	0.10	0.20	3.53	28.20	5.00
1946897	5.32	19.10	72.70	2.63	10.70	10.68	0.17	4.29	513.50	6.10	3.00	0.52	0.01	0.80	3.23	54.10	469.40	15.00
1946899	3.82	23.00	4.53	1.38	4.50	0.84	0.02	4.49	43.10	22.70	0.40	1.87	0.01	0.20	0.86	17.60	34.10	26.00
1947185	2.99	18.00	4.56	0.79	2.90	0.86	0.06	3.25	32.30	21.40	0.32	0.77	0.01	0.90	2.36	7.70	24.80	8.00
1960848	4.08	4.30	9.68	0.80	3.80	1.53	0.01	2.51	56.50	6.50	0.46	0.35	0.01	1.50	0.52	8.45	54.60	66.00
1933087	3.61	19.00	12.66	1.11	7.30	3.03	0.02	3.52	107.00	23.60	1.80	0.91	0.02	0.30	0.28	56.50	70.70	2.00
1960879	3.39	5.50	2.59	0.40	1.20	0.42	0.04	1.19	15.30	31.00	0.15	15.22	0.80	3.50	0.11	2.91	12.00	47.00
1933072	8.09	17.40	11.35	1.29	9.50	1.73	0.05	5.00	106.70	26.50	0.64	4.36	0.18	0.50	0.16	18.70	72.00	17.00
1960842	3.61	8.00	4.85	0.40	5.40	1.26	0.04	2.33	21.50	5.70	0.55	11.59	0.18	14.90	1.37	7.88	19.50	47.00
1933077	3.08	8.50	3.10	0.33	7.20	0.81	0.00	3.14	9.80	10.30	0.46	0.54	0.01	0.40	1.22	7.40	10.10	10.00
1949033	7.72	16.30	4.43	0.88	7.80	0.67	0.12	3.65	29.10	35.60	0.32	1.92	0.17	1.30	0.10	8.92	22.70	12.00
1949031	4.00	8.10	51.27	0.55	7.20	12.53	0.05	1.31	268.00	27.10	3.16	3.57	0.03	0.90	1.92	7.89	215.60	7.00
1949046	2.86	3.80	2.56	0.89	2.20	0.58	0.01	2.32	20.80	15.50	0.26	0.53	0.02	0.20	0.22	2.23	17.80	0.05
1949829	4.57	12.90	5.07	0.40	4.30	0.84	0.04	4.84	54.30	24.60	0.41	1.74	0.05	0.40	0.11	8.68	37.50	25.00
1960890	3.54	6.40	2.31	0.50	2.50	0.41	0.00	2.69	23.90	16.40	0.17	1.05	0.03	0.20	0.06	3.03	16.30	13.00
1960893	5.41	8.60	4.13	1.00	2.90	0.71	0.02	4.05	40.60	16.80	0.28	1.00	0.04	0.30	0.12	4.76	29.10	19.00
1949824	7.17	11.20	4.37	0.90	8.30	0.61	0.03	2.63	26.00	40.40	0.34	2.74	0.01	0.40	1.70	8.77	22.90	26.00
1937382	4.67	8.00	3.45	1.28	5.20	0.62	0.06	4.59	54.20	11.10	0.27	0.30	0.01	0.50	0.09	11.30	25.90	8.00
1937179	9.03	15.80	3.77	1.58	4.00	0.72	0.03	5.07	35.30	25.70	0.37	2.46	0.05	0.40	0.42	8.00	27.00	25.00
0000004	3.96	9.30	3.71	0.40	2.50	0.80	0.05	2.21	25.50	13.00	0.31	15.69	0.26	0.30	0.56	8.22	19.60	47.00
1949007	4.26	3.20	2.18	0.10	0.70	0.39	0.03	0.67	13.80	6.80	0.14	14.46	0.89	11.40	0.04	2.95	8.90	19.00
1937391	3.03	8.30	3.37	0.97	2.70	0.65	0.05	3.09	19.70	30.50	0.26	12.93	0.30	2.10	0.12	4.40	18.70	3.00

Table 2c: Whole rock geochemistry for samples 1937885 to 1937391 (inclusive), elements P_2O_5 - Th

Samp_R#	P2O5 (wt%)	Pb (ppm)	Pd (ppm)	Pr (ppm)	Pt (ppb)	Rb (ppm)	Re (ppm)	S (ppm)	Sb (ppm)	Sc (ppm)	Se (ppm)	SiO2 (wt%)	Sm (ppm)	Sn (ppm)	Sr (ppm)	Ta (ppm)	Tb (ppm)	Te (ppm)	Th (ppm)
1960885	0.15	32.00	2.00	10.70	2.00	245.50	0.00	181.00	0.63	20.00	0.03	69.29	6.96	4.00	24.80	1.60	0.74	0.05	13.71
1949036	0.05	6.00	0.05	55.51	0.05	70.60	0.00	170.00	0.49	10.00	2.10	78.02	36.47	2.00	67.40	1.60	2.77	0.12	16.75
1949788	0.20	9.00	0.05	12.92	0.05	179.80	0.00	144.00	0.63	15.00	2.10	71.04	9.79	4.00	19.40	1.50	1.89	0.36	14.79
1949793	0.29	2.50	0.05	21.52	0.05	174.50	0.00	83.00	0.28	10.00	0.90	69.22	13.97	6.00	15.50	1.70	0.94	0.11	21.43
1960888	0.03	2.50	0.05	6.36	0.05	50.10	0.00	25.00	0.20	1.00	0.03	93.70	3.94	2.00	12.90	0.40	0.35	0.05	10.42
1949784	0.10	7.00	0.05	2.60	0.05	95.00	0.01	153.00	0.22	10.00	1.00	89.40	1.92	3.00	25.80	0.60	0.75	0.05	6.46
1949039	0.17	9.00	0.05	11.40	0.05	242.40	0.01	968.00	0.37	16.00	0.03	64.14	8.24	5.00	51.30	1.70	0.98	0.16	18.20
1949796	0.18	7.00	0.05	9.23	0.05	214.00	0.00	1405.00	1.95	17.00	3.00	65.92	6.73	4.00	38.60	1.40	0.74	0.28	16.46
1949821	0.20	10.00	0.05	10.63	4.00	230.80	0.00	1406.00	1.44	12.00	0.03	57.88	7.59	5.00	32.50	1.70	0.95	0.05	20.48
1949016	0.15	36.00	1.00	7.06	1.00	234.00	0.00	5847.00	1.62	19.00	0.03	60.65	5.28	4.00	37.00	1.40	0.69	0.16	13.90
1949022	0.13	21.00	0.05	6.96	1.00	204.70	0.01	2722.00	0.86	22.00	7.40	58.61	5.46	4.00	28.40	1.50	0.86	0.17	13.96
1937184	0.22	2.50	0.05	11.44	0.05	115.20	0.00	2009.00	0.28	14.00	4.00	64.01	7.77	3.00	40.30	2.40	0.85	0.20	26.14
1949814	0.12	8.00	4.00	7.87	1.00	151.50	0.00	346.00	0.23	1.00	0.03	82.75	4.89	2.00	19.10	1.10	0.56	0.05	13.11
0000001	0.16	13.00	0.05	9.64	0.05	140.50	0.00	682.00	0.28	21.00	0.03	60.18	7.10	4.00	116.00	1.60	0.88	0.05	16.07
1937388	0.05	5.00	0.05	3.96	0.05	47.10	0.00	145.00	0.25	10.00	2.70	85.25	3.02	3.00	12.90	1.60	0.53	0.05	9.40
1949790	0.13	8.00	0.05	8.67	0.05	153.00	0.00	86.00	0.34	10.00	3.10	83.92	5.96	2.00	105.70	0.60	0.58	0.08	14.77
1949012	0.04	11.00	0.05	7.65	0.05	131.70	0.00	361.00	0.27	10.00	3.20	79.80	5.68	2.00	20.60	0.70	0.74	0.05	10.40
1946897	0.20	32.00	0.05	127.80	0.05	258.10	0.01	161.00	0.23	31.00	3.80	63.09	95.02	10.00	134.40	4.80	10.12	0.05	20.39
1946899	0.04	5.00	0.05	9.65	0.05	618.20	0.00	177.00	0.09	15.00	2.70	63.09	5.98	4.00	75.00	1.70	0.64	0.05	28.54
1947185	0.02	8.00	0.05	6.75	0.05	157.80	0.00	208.00	0.31	10.00	4.40	67.12	4.78	2.00	73.00	0.80	0.69	0.08	13.03
1960848	0.19	12.00	0.05	14.05	10.00	75.30	0.00	104.00	0.18	1.00	0.03	86.44	10.99	1.00	28.00	0.80	1.34	0.70	11.94
1933087	0.12	2.50	0.05	20.68	0.05	358.60	0.00	149.00	0.80	10.00	0.90	75.03	14.25	10.00	14.20	7.10	2.02	0.05	86.74
1960879	0.09	7.00	0.05	3.15	0.05	40.20	0.00	7228.00	1.14	1.00	0.03	19.55	2.62	0.05	57.20	0.30	0.36	0.05	4.00
1933072	0.15	6.00	0.05	19.46	1.00	264.90	0.00	411.00	0.90	11.00	4.00	54.90	13.61	10.00	32.10	2.40	1.60	0.20	39.05
1960842	0.09	148.00	0.05	5.08	2.00	78.50	0.00	426.00	1.01	1.00	0.03	33.48	4.41	2.00	91.90	0.90	0.83	0.05	5.60
1933077	0.13	6.00	0.05	2.36	0.05	96.00	0.00	25.00	0.14	10.00	5.30	83.44	2.49	4.00	31.50	1.00	0.50	0.05	11.33
1949033	0.20	15.00	0.05	6.11	0.05	261.10	0.00	3197.00	2.67	12.00	1.60	71.63	4.77	3.00	19.10	1.00	0.59	0.07	12.80
1949031	0.24	2.50	0.05	58.52	0.05	42.10	0.00	94.00	0.07	10.00	2.50	73.08	49.35	3.00	29.90	1.50	9.13	0.14	23.14
1949046	0.08	6.00	0.05	5.12	0.05	82.40	0.00	25.00	0.09	10.00	2.60	89.49	3.45	1.00	49.30	0.30	0.40	0.05	9.60
1949829	0.08	15.00	1.00	10.47	4.00	242.60	0.00	228.00	0.55	1.00	0.03	75.67	6.71	3.00	26.70	1.10	0.69	0.20	14.03
1960890	0.06	2.50	0.05	4.67	0.05	99.20	0.00	196.00	0.18	1.00	0.03	86.49	2.91	2.00	14.60	0.80	0.32	0.05	6.99
1960893	0.07	11.00	0.05	8.02	0.05	163.20	0.00	171.00	0.15	1.00	0.03	78.76	5.44	3.00	27.30	1.40	0.62	0.10	10.25
1949824	0.15	7.00	0.05	5.90	6.00	102.70	0.00	171.00	0.51	1.00	0.03	74.42	4.69	4.00	25.50	1.10	0.54	0.05	13.66
1937382	0.23	10.00	0.05	7.98	0.05	166.70	0.03	79.00	0.65	10.00	4.70	80.62	4.03	2.00	39.50	0.70	0.46	0.05	12.32
1937179	0.19	5.00	0.05	7.32	1.00	179.90	0.00	212.00	0.39	16.00	2.70	70.73	4.84	11.00	18.30	1.30	0.52	0.11	11.28
0000004	0.01	2.50	0.05	5.45	0.05	58.40	0.00	207.00	0.30	1.00	0.03	21.01	3.89	2.00	52.30	0.90	0.57	0.05	9.33
1949007	0.07	20.00	0.05	2.31	0.05	27.20	0.01	11244.00	2.63	10.00	2.60	17.80	2.03	0.05	62.70	0.30	0.31	0.05	3.39
1937391	0.13	2.50	0.05	4.53	0.05	116.30	0.00	88.00	0.28	10.00	0.90	26.36	3.97	2.00	104.90	0.70	0.50	0.20	7.12

Table 2d: Whole rock geochemistry for samples 1937885 to 1937391 (inclusive), elements TiO_2 - Zr

Samp_R#	TiO2 (wt%)	Tl (ppm)	Tm (ppm)	U (ppm)	V (ppm)	W (ppm)	Y (ppm)	Yb (ppm)	Zn (ppm)	Zr (ppm)
1960885	0.91	0.58	0.32	3.49	128.00	26.00	25.90	2.26	87.00	133.00
1949036	0.29	0.25	1.05	7.49	25.00	1.00	82.50	6.63	116.00	237.00
1949788	0.78	0.44	0.74	5.57	107.00	21.00	69.30	4.10	145.00	149.00
1949793	0.46	0.42	0.56	5.90	50.00	3.00	34.00	4.02	16.00	316.00
1960888	0.10	0.19	0.17	1.59	11.00	1.00	13.20	1.29	0.05	116.00
1949784	0.10	0.49	0.62	1.87	17.00	1.00	54.40	3.41	9.00	71.00
1949039	0.75	1.22	0.54	3.57	86.00	3.00	35.90	3.40	92.00	222.00
1949796	0.79	0.98	0.46	3.39	113.00	4.00	28.50	2.93	57.00	217.00
1949821	0.65	0.64	0.53	2.87	84.00	4.00	35.00	3.41	23.00	250.00
1949016	0.72	1.76	0.43	3.34	120.00	4.00	26.20	2.76	66.00	203.00
1949022	0.77	1.07	0.51	3.37	145.00	6.00	32.10	3.29	49.00	199.00
1937184	0.66	0.36	0.68	6.00	112.00	4.00	38.10	3.87	31.00	346.00
1949814	0.34	0.50	0.31	3.50	42.00	7.00	21.60	2.08	70.00	134.00
0000001	0.98	0.82	0.44	4.30	188.00	2.00	29.50	2.85	209.00	168.00
1937388	0.85	0.27	0.36	2.08	72.00	5.00	22.60	2.21	15.00	304.00
1949790	0.22	0.64	0.25	4.21	19.00	4.00	17.90	1.62	28.00	106.00
1949012	0.33	0.72	0.38	1.94	21.00	4.00	30.40	2.22	23.00	117.00
1946897	0.79	0.97	3.75	19.27	113.00	6.00	260.90	22.31	101.00	366.00
1946899	0.58	1.42	0.36	3.26	73.00	1.00	23.80	2.49	61.00	169.00
1947185	0.28	0.37	0.30	1.26	59.00	2.00	22.60	1.96	23.00	101.00
1960848	0.16	0.33	0.52	5.60	27.00	3.00	49.00	3.15	7.00	144.00
1933087	0.29	0.81	1.51	16.42	24.00	0.05	87.50	10.53	22.00	225.00
1960879	0.15	2.11	0.12	2.79	16.00	3.00	12.80	0.97	32.00	47.00
1933072	0.78	0.60	0.64	5.92	81.00	11.00	51.60	3.90	21.00	331.00
1960842	0.33	6.25	0.54	3.65	25.00	0.05	36.90	3.64	34.00	204.00
1933077	0.32	0.36	0.43	2.92	25.00	1.00	25.50	2.57	21.00	285.00
1949033	0.40	2.10	0.30	14.56	46.00	6.00	20.10	1.90	113.00	324.00
1949031	0.31	0.13	4.16	9.91	46.00	1.00	479.60	22.28	182.00	266.00
1949046	0.19	0.40	0.27	1.40	24.00	3.00	17.20	1.66	47.00	84.00
1949829	0.46	0.80	0.33	3.37	50.00	9.00	26.00	2.47	99.00	156.00
1960890	0.29	0.38	0.12	1.62	26.00	6.00	11.80	1.04	19.00	103.00
1960893	0.42	0.57	0.25	2.52	53.00	10.00	21.50	1.81	11.00	111.00
1949824	0.41	0.30	0.24	2.40	36.00	3.00	18.30	1.86	17.00	314.00
1937382	0.38	0.62	0.26	2.82	47.00	3.00	16.60	1.76	11.00	199.00
1937179	0.71	0.99	0.38	5.29	96.00	8.00	21.20	2.09	47.00	136.00
0000004	0.30	0.22	0.33	1.50	23.00	2.00	24.50	2.09	32.00	91.00
1949007	0.17	1.55	0.15	2.71	21.00	3.00	11.60	0.99	9.00	29.00
1937391	0.36	0.45	0.30	2.39	81.00	1.00	19.30	1.45	41.00	108.00

APPENDIX C: ELEMENTAL MAPS (SEM IMAGES)

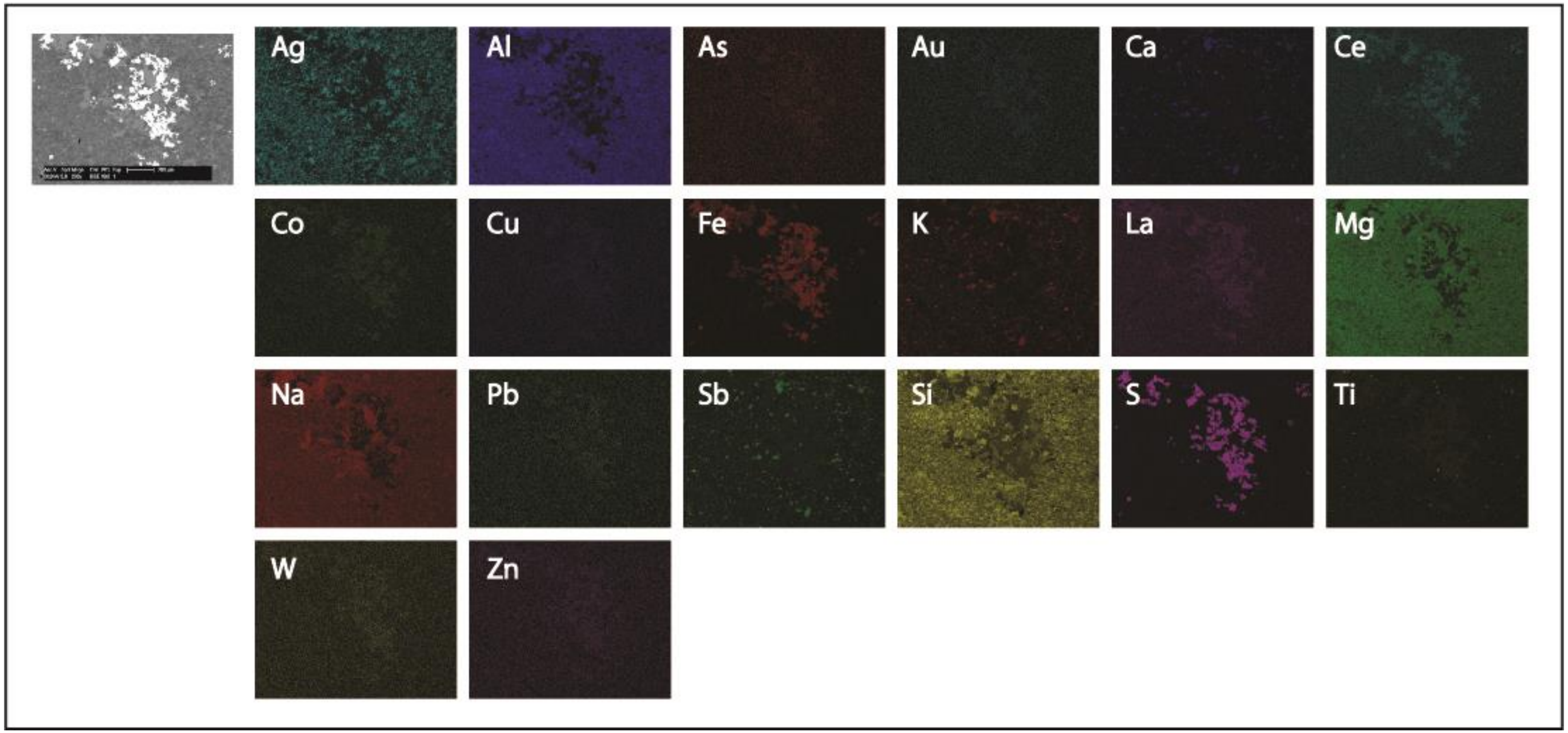

Figure 1a) BSE image and elemental maps of sample 1949016 (diamictite), Map 1

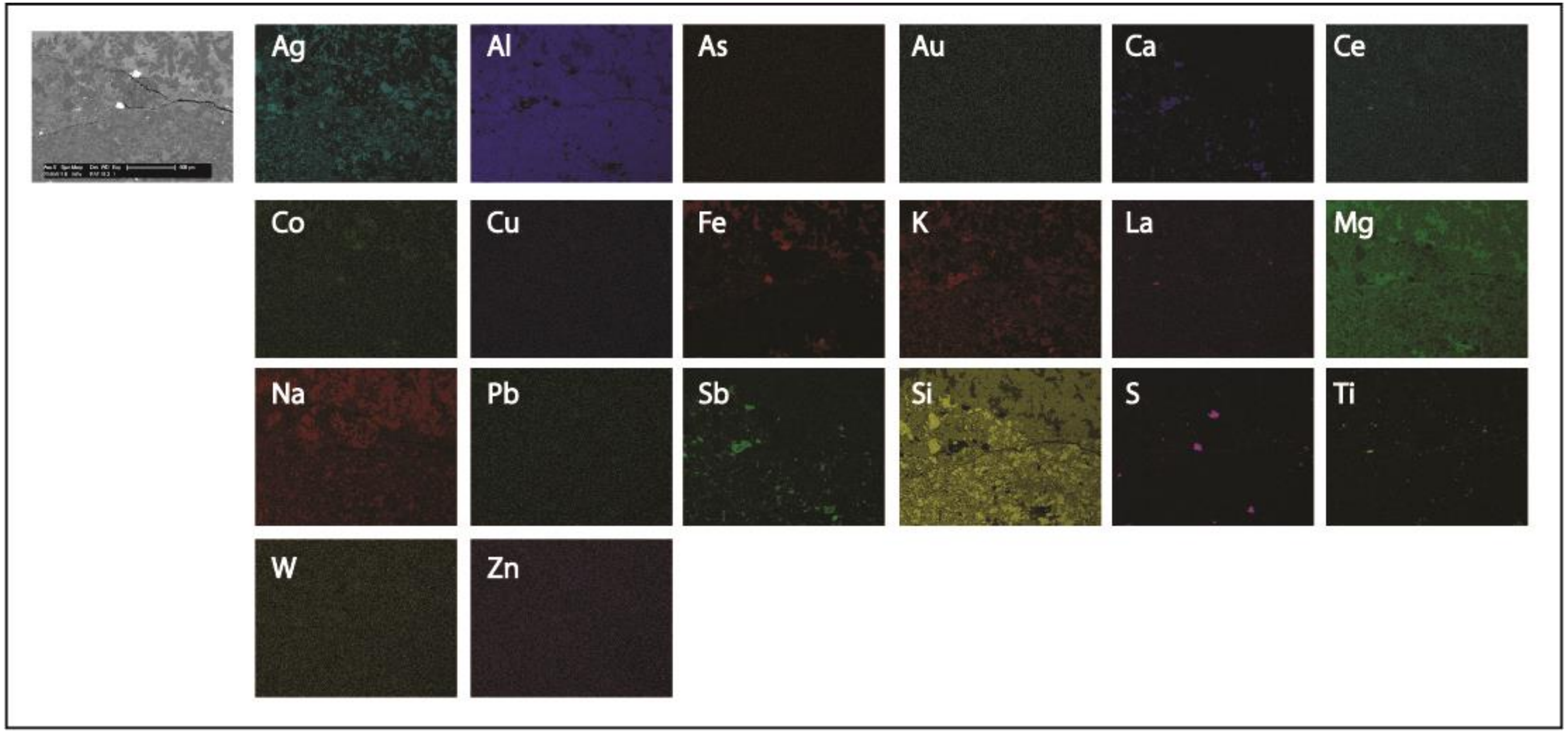

Figure 1b) BSE image and elemental maps of sample 1949016 (diamictite), Map 2

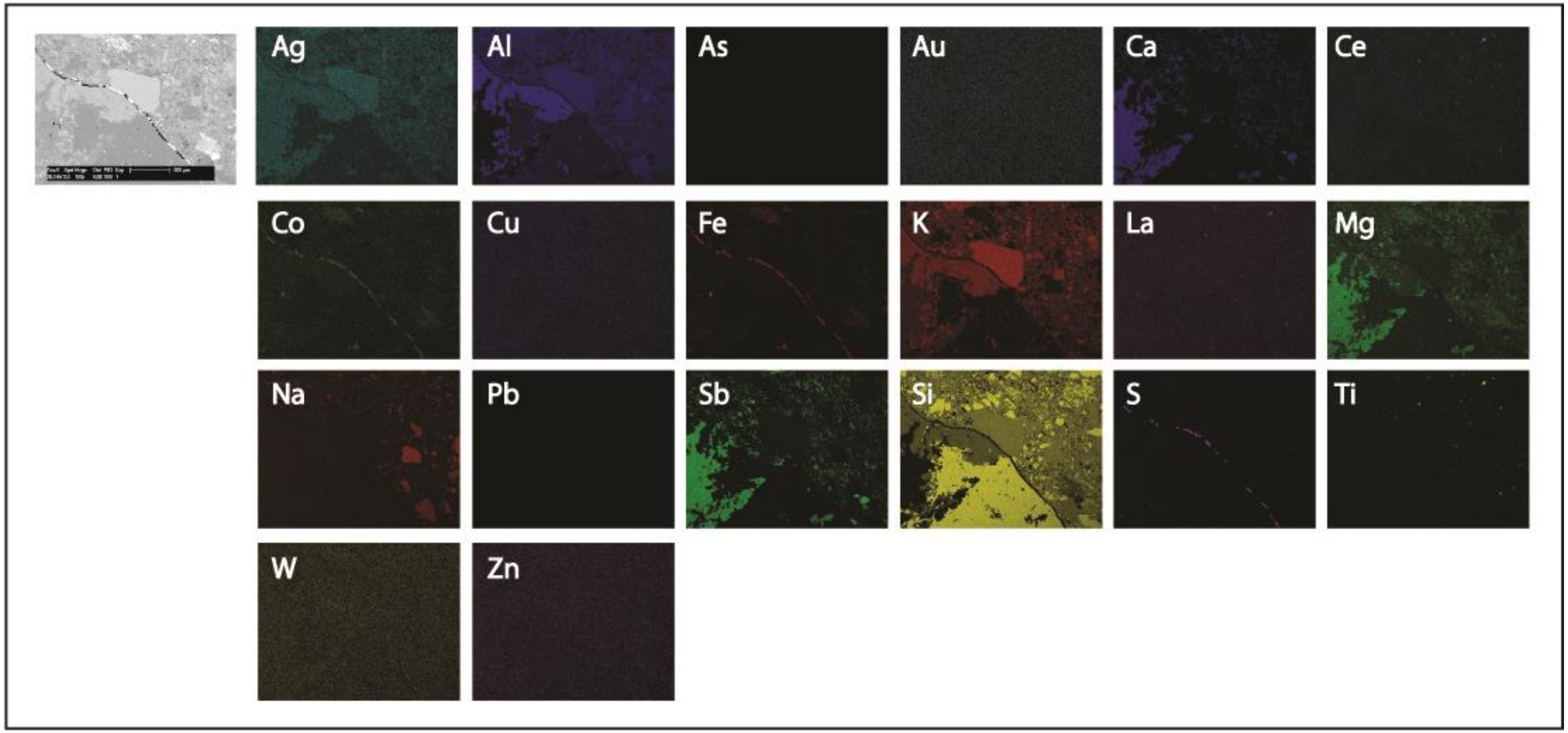

Figure 2a) BSE image and elemental maps of sample 1949022 (diamictite), Map 1

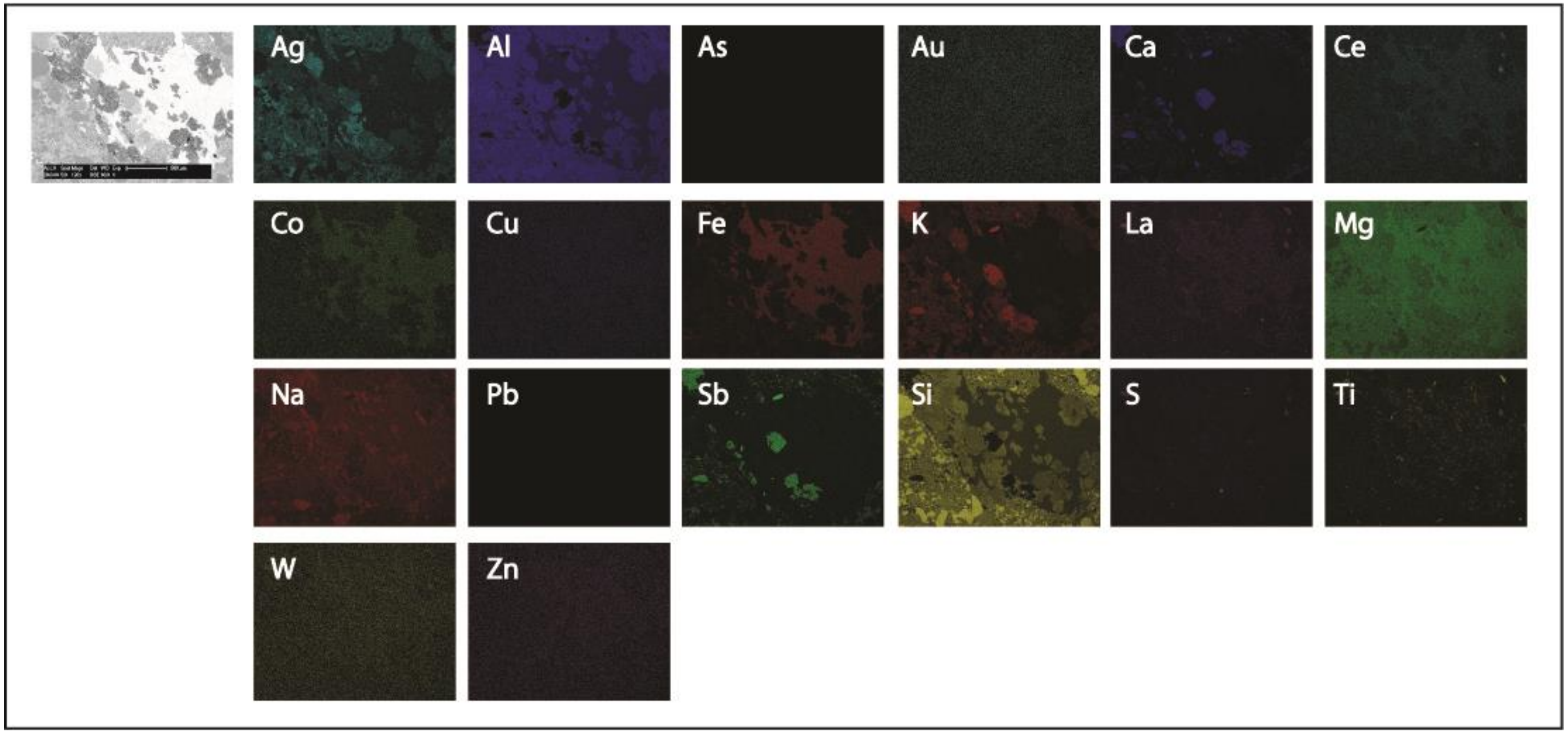

Figure 2b) BSE image and elemental maps of sample 1949022 (diamictite), Map 2

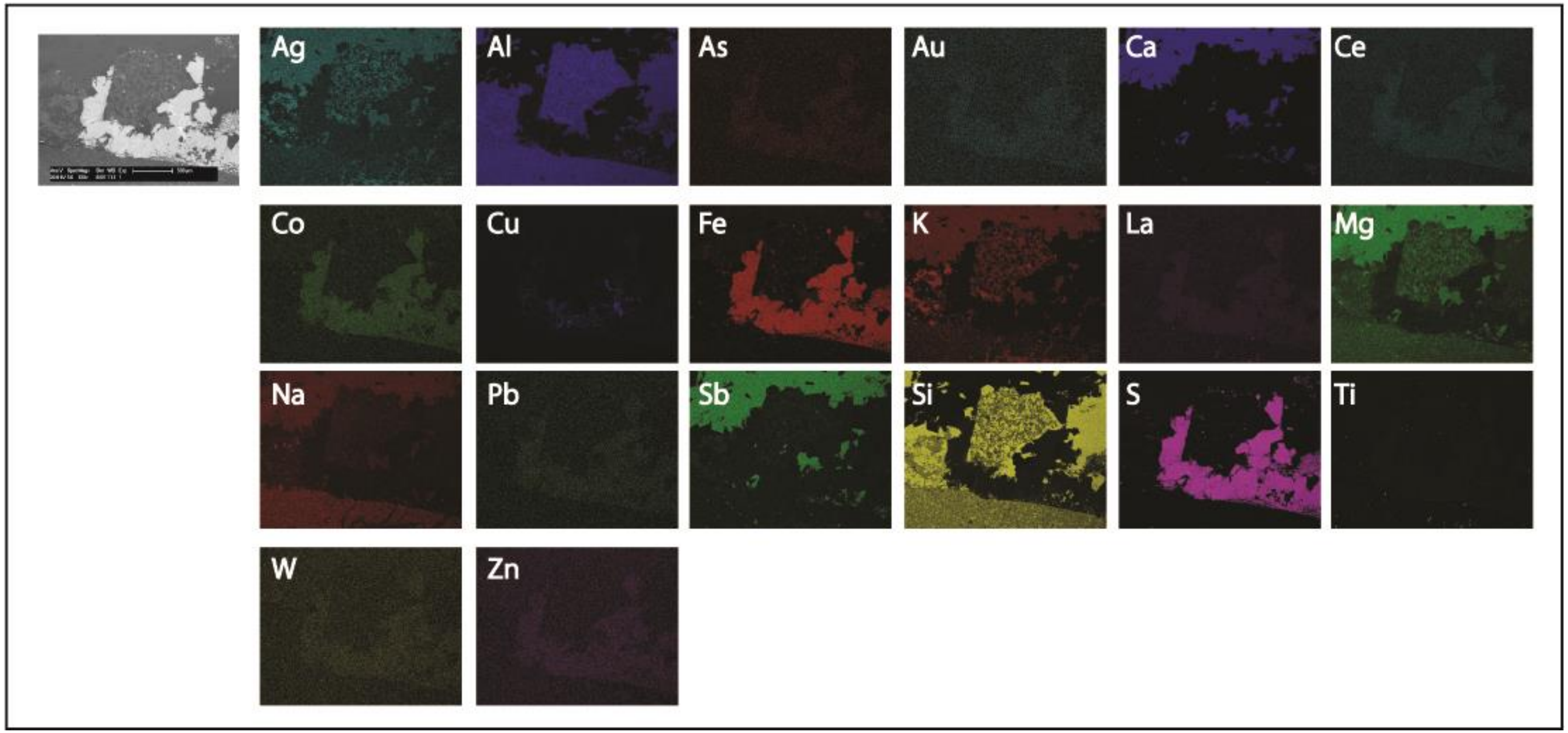

Figure 3a) BSE image and elemental maps of sample 1960882 (conglomerate), Map 1

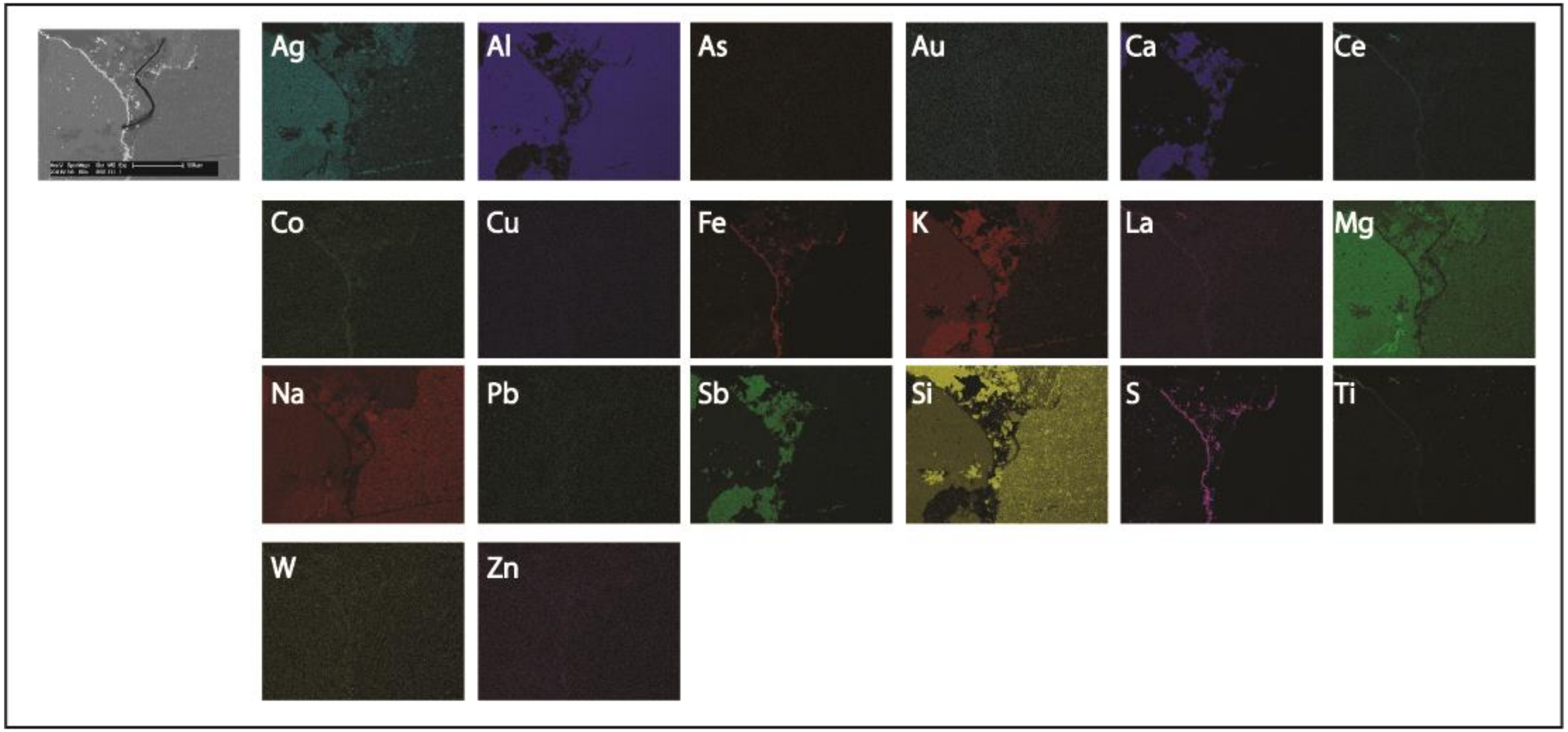

Figure 3b) BSE image and elemental maps of sample 1960882 (conglomerate), Map 2

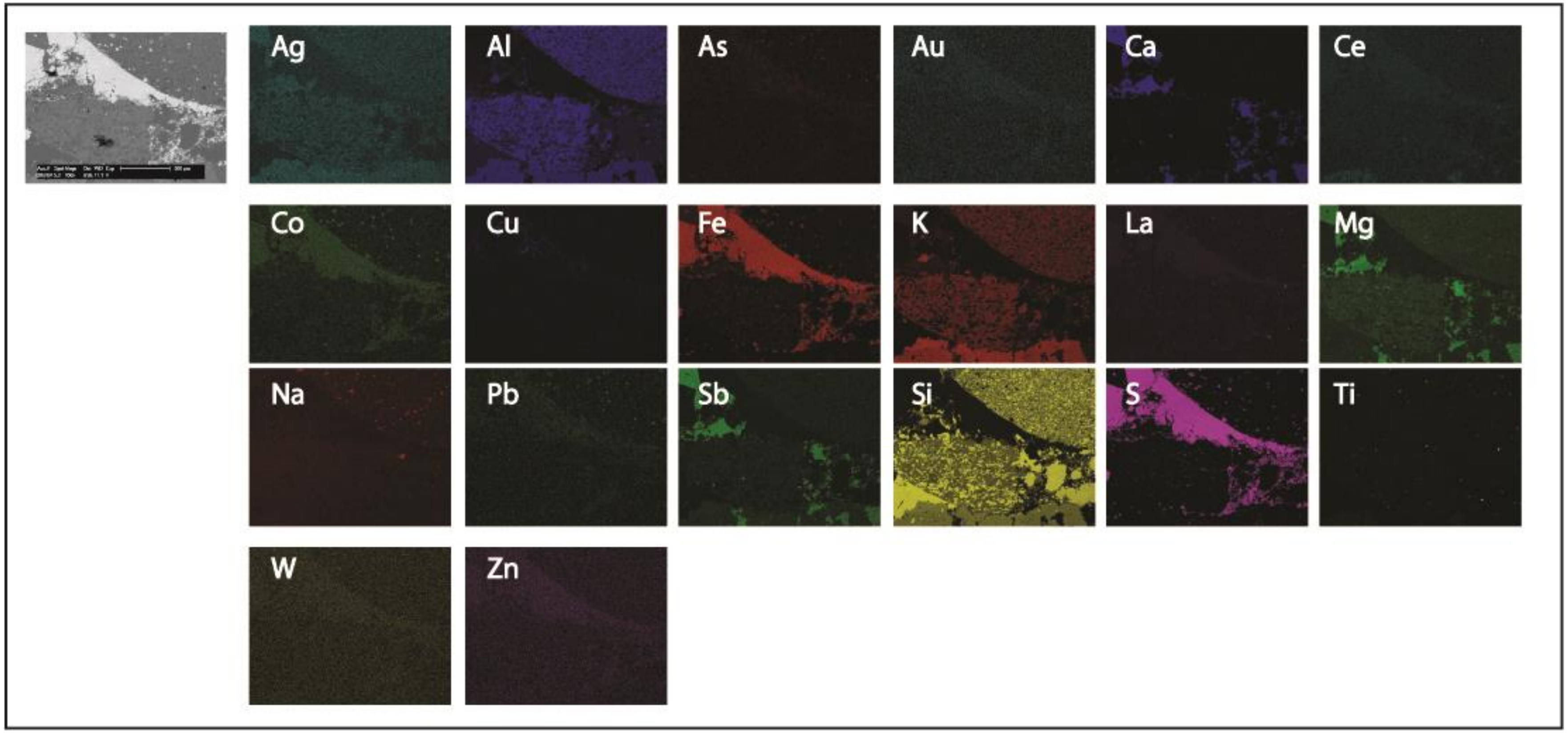

Figure 3c) BSE image and elemental maps of sample 1960882 (conglomerate), Map 3

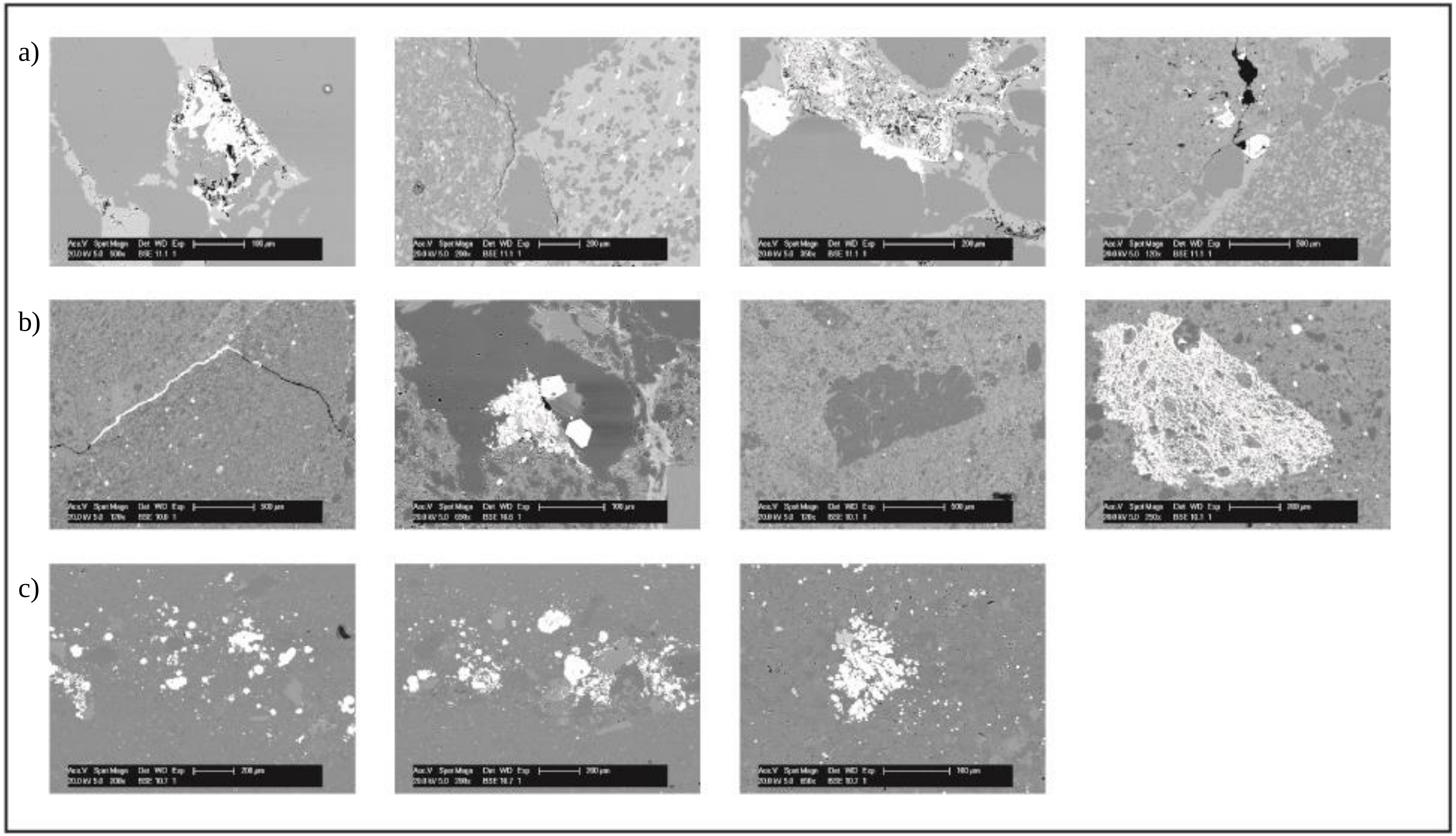

Figure 4: BSE images of samples a) 1949814 (diamictite); b) 1949821 (diamictite); c) 1949025 (carbonate)

APPENDIX D: LA-ICP-MS DATA

Table 1a: LA-ICP-MS data for elements Na - Mo

Sample_No	Text	Na (ppm)	Si (ppm)	S (ppm)	V (ppm)	Cr (ppm)	Mn (ppm)	Fe (ppm)	Co (ppm)	Ni (ppm)	Cu (ppm)	Zn (ppm)	Ga (ppm)	As (ppm)	Se (ppm)	Mo (ppm)
016101	P	63.550	0.000	520423	1.980	1.870	5.680	465500	2051.38	371.160	741.460	0.000	0.178	678.66	22.590	0.360
016102	P	1267.76	0.000	517771	27.040	17.200	202.390	465500	1545.04	170.140	797.760	54.200	3.480	3323.96	18.790	1.090
016103	P	822.400	0.000	541090	132.600	78.510	589.110	465500	1590.01	208.810	1133.23	62.880	14.290	305.61	0.000	1.340
016104	P	178.510	0.000	515746	28.900	37.270	57.020	465500	1082.89	423.480	1874.16	8.830	2.210	712.82	14.410	10.700
016105	P	1483.20	0.000	525841	63.250	27.300	25.550	465500	1188.08	1071.89	300.070	1054.9	11.760	500.92	52.660	2.760
016201	P	180.360	0.000	559227	1.930	0.000	2.760	465500	694.830	1402.24	182.410	1.330	0.448	207.60	17.920	17.440
016202	P	168.340	0.000	554637	1.690	0.000	1.850	465500	605.160	1447.13	96.570	0.000	0.233	115.82	13.310	6.110
016203	P	856.260	0.000	529592	27.970	11.770	10.700	465500	793.050	1453.54	2588.15	17.890	5.640	306.49	19.390	11.650
016204	P	119.180	0.000	523116	2.280	1.570	2.460	465500	714.800	1710.74	132.950	7.670	0.159	165.49	33.150	8.630
016205	P	183.130	0.000	517108	5.270	2.550	3.260	465500	733.640	1979.85	123.190	3.590	1.020	115.54	39.100	5.290
016206	P	215.100	0.000	510945	0.890	0.000	3.680	465500	347.270	758.170	47.460	1.960	0.184	74.53	15.290	0.980
882101	S	796.190	0.000	575873	215.120	53.110	1394.05	465500	2199.93	1416.21	452.160	47.590	818.050	4131.01	0.000	13.560
882102	S	782.310	0.000	595018	175.910	40.490	1369.33	465500	1777.57	1229.43	362.430	33.940	604.640	4059.44	0.000	8.020
882103	S	680.980	0.000	526538	191.370	45.090	938.910	465500	1766.27	1334.76	147.510	14.140	459.940	3068.90	0.000	8.610
882104	S	545.050	0.000	541521	152.750	37.400	877.520	465500	1877.76	1372.63	71.730	16.400	367.300	2735.83	0.000	4.900
882201	S	10.740	0.000	509840	0.000	0.000	5.110	465500	7.790	10.850	245.610	1.810	0.000	1186.68	0.000	2.460
882202	S	16.660	0.000	500633	0.162	0.000	17.290	465500	61.690	40.650	421.980	1.820	0.000	2329.35	0.000	28.760
882203	S	0.000	0.000	491941	0.279	0.000	17.260	465500	52.360	31.830	264.630	1.670	0.000	6613.64	0.000	17.050
882204	S	11.760	0.000	520046	0.210	0.000	13.340	465500	14.830	9.410	27.630	0.000	0.000	17075.7	0.000	8.880
882205	S	0.000	0.000	536616	0.111	0.000	8.980	465500	1.670	1.500	6.880	1.320	0.000	13901.8	0.000	4.300
882211	S	0.000	0.000	512486	0.373	0.000	17.730	465500	15.620	15.680	21.110	3.930	0.000	12333.2	0.000	10.630
882212	S	18.910	0.000	518963	1.380	1.300	18.830	465500	89.570	38.320	168.190	5.050	0.406	13535.5	0.000	13.870
882213	S	38.670	0.000	501962	0.000	0.000	4.840	465500	32.420	12.840	42.250	1.390	0.000	15435.6	0.000	30.120
882214	S	0.000	0.000	510418	0.279	0.000	32.820	465500	29.140	8.740	107.560	2.290	0.000	17403.8	0.000	17.010
882215	S	0.000	0.000	514329	0.495	0.000	55.050	465500	196.390	86.450	251.950	0.000	0.000	3208.47	0.000	59.310
882216	S	0.000	0.000	483958	0.000	0.000	8.380	465500	4.210	8.130	7.750	0.000	0.000	18665.9	0.000	13.310
882217	S	0.000	0.000	515148	0.217	0.000	10.010	465500	3.820	4.430	22.980	2.560	0.000	17282.2	0.000	34.620
882218	S	0.000	0.000	483606	0.214	0.000	27.440	465500	13.790	11.770	64.120	0.000	0.000	6837.85	0.000	21.030
882219	S	0.000	0.000	527416	0.215	0.000	49.310	465500	50.890	28.760	457.770	0.000	0.000	4691.41	0.000	30.100
882220	S	0.000	0.000	489780	0.121	0.000	8.360	465500	58.980	22.570	25.110	1.950	0.000	7918.85	0.000	26.340
882221	S	19.170	0.000	503212	0.243	0.000	8.070	465500	89.910	41.220	532.250	0.000	0.099	2410.90	0.000	4.020

Table 1b: LA-ICP-MS data for elements Ag - Bi

Sample_No	Ag (ppm)	Cd (ppm)	In (ppm)	Sn (ppm)	Sb (ppm)	Te (ppm)	Ba (ppm)	W (ppm)	Ir (ppm)	Au (ppm)	Hg (ppm)	Tl (ppm)	Pb (ppm)	Bi (ppm)
016101	3.360	0.000	0.036	6.340	5.540	0.000	54.710	0.000	0.000	0.000	0.082	39.960	81.210	3.700
016102	3.470	0.000	0.029	5.140	5.620	0.850	510.720	0.337	0.000	0.162	0.078	26.400	82.920	10.540
016103	6.620	0.000	0.121	14.030	13.590	1.470	2893.89	1.430	0.000	0.102	0.000	56.750	158.320	11.530
016104	16.920	0.000	0.064	4.470	10.480	0.920	322.930	2.170	0.000	0.075	3.150	175.130	350.130	14.990
016105	2.040	0.690	0.850	2.230	5.520	1.490	6140.35	2.190	0.000	0.000	0.000	8.460	46.700	17.480
016201	5.340	0.000	0.080	0.830	6.910	1.100	354.470	0.000	0.000	0.045	0.000	8.790	591.350	60.740
016202	4.480	0.000	0.111	0.000	3.510	0.680	168.030	0.214	0.000	0.000	0.000	16.480	719.800	48.380
016203	14.600	0.000	0.100	1.010	6.450	0.990	3093.62	1.290	0.000	0.069	0.000	48.100	991.550	63.740
016204	16.520	0.000	0.090	0.000	7.350	2.040	202.420	0.620	0.000	0.091	0.049	47.600	888.450	57.250
016205	8.030	0.000	0.060	0.000	4.570	1.490	586.070	0.212	0.000	0.063	0.000	14.330	717.540	48.500
016206	3.560	0.000	0.056	0.200	1.640	1.310	101.070	0.000	97.000	0.057	0.000	15.350	777.680	12.580
882101	28.940	0.000	0.116	11.980	45.160	0.000	0.000	4.580	0.000	0.000	0.000	118.850	689.120	2.500
882102	22.130	0.600	0.111	9.870	44.460	0.000	0.000	5.780	0.000	0.000	0.201	135.900	696.960	0.304
882103	12.350	0.000	0.085	12.570	34.330	0.000	0.000	9.570	0.000	0.000	0.150	136.230	427.670	0.260
882104	10.590	0.780	0.099	8.660	27.320	0.000	0.000	5.180	0.000	0.000	0.000	105.410	308.240	0.238
882201	12.670	0.000	0.000	0.000	480.230	0.000	0.000	0.000	0.000	0.000	0.000	14.720	974.280	0.000
882202	19.400	0.570	0.000	0.330	483.000	0.000	1.980	0.000	0.000	0.000	0.000	39.210	0.000	0.145
882203	16.730	0.400	0.000	0.000	309.850	0.000	5.110	0.000	0.000	0.000	0.000	31.530	854.140	0.263
882204	9.660	0.000	0.000	0.000	25.380	0.000	0.000	0.000	0.000	0.000	0.055	59.940	854.640	0.539
882205	9.830	0.000	0.000	0.000	16.370	0.000	0.000	0.000	0.000	0.000	0.000	25.420	408.090	0.000
882211	9.050	0.000	0.000	0.000	9.990	0.000	46.760	0.000	0.000	0.000	0.000	57.180	152.710	0.336
882212	11.470	0.000	0.000	0.360	40.090	0.000	14.060	0.050	0.000	0.000	0.000	32.530	626.700	1.590
882213	13.480	0.000	0.015	0.000	35.160	0.000	2.240	0.000	0.000	0.000	0.000	35.540	1105.71	0.463
882214	13.460	0.000	0.000	0.000	41.590	0.000	7.260	0.000	0.000	0.000	0.000	53.690	939.620	0.257
882215	7.830	0.000	0.000	0.000	486.370	0.000	4.810	0.000	0.000	0.000	0.000	30.800	996.340	0.317
882216	16.430	0.000	0.000	0.000	58.980	0.000	0.000	0.000	0.000	0.000	0.000	123.660	752.850	0.146
882217	11.650	0.000	0.000	0.220	39.760	0.000	2.300	0.000	0.000	0.000	0.000	17.260	1181.96	0.000
882218	11.640	0.330	0.000	0.000	71.340	0.000	2.510	0.000	0.000	0.000	0.000	68.640	1043.51	0.024
882219	16.460	0.650	0.000	0.330	665.720	0.000	3.830	0.064	0.000	0.000	0.000	49.580	1169.46	0.124
882220	12.830	0.000	0.000	0.240	13.500	0.000	1.900	0.000	0.000	0.000	0.000	34.260	211.650	0.870
882221	32.530	0.000	0.017	0.500	828.170	0.000	7.530	0.000	0.000	0.000	0.000	27.280	0.000	1.020

Table 2a: LA-ICP-MS data for standards, elements Na - Mo

Sample_No	Na (ppm)	Si (ppm)	S (ppm)	V (ppm)	Cr (ppm)	Mn (ppm)	Fe (ppm)	Co (ppm)	Ni (ppm)	Cu (ppm)	Zn (ppm)	Ga (ppm)	As (ppm)	Se (ppm)	Mo (ppm)
STDM-01	35391.8	0.000	271388	62.180	66.290	275.900	156000	57.240	96.450	128010	205675	63.850	64.900	57.980	58.970
STDM-02	35531.5	0.000	272961	61.440	63.580	276.090	156000	61.060	97.170	131479	215474	63.490	62.830	45.750	56.870
STDM-03	27637.2	0.000	273254	62.310	62.550	285.100	156000	59.190	94.850	133862	211162	63.860	68.590	52.960	58.380
STDM-04	33759.3	0.000	302814	62.500	67.440	284.720	156000	61.810	102.050	144534	222233	64.170	63.970	47.920	62.110
STDM-05	34316.1	0.000	283206	65.060	65.710	295.030	156000	63.720	98.600	139439	217315	64.140	66.040	61.100	62.770
STDM-06	38832.4	0.000	253865	62.150	63.840	252.070	156000	54.670	90.480	132364	190645	64.210	63.220	49.040	53.540
STDM-07	31036.9	0.000	262818	63.610	64.570	260.150	156000	58.530	94.710	129244	195584	65.900	62.850	43.730	57.570
STDM-08	34980.1	0.000	291667	63.950	64.650	284.680	156000	61.420	96.430	137006	210794	63.160	65.350	35.130	63.150
STDM-09	38410.8	0.000	260950	64.240	68.290	281.330	156000	60.030	96.390	129313	205829	65.190	64.250	46.080	56.670

Table 2b: LA-ICP-MS data for standards, elements Ag - Bi

Sample_No	Ag (ppm)	Cd (ppm)	In (ppm)	Sn (ppm)	Sb (ppm)	Te (ppm)	Ba (ppm)	W (ppm)	Ir (ppm)	Au (ppm)	Hg (ppm)	Tl (ppm)	Pb (ppm)	Bi (ppm)
STDM-01	48.980	60.630	51.070	60.360	60.550	13.630	17.620	20.990	42.940	53.890	63.900	51.970	67.010	60.560
STDM-02	49.320	59.940	53.680	58.670	59.960	15.070	16.680	20.200	41.510	56.190	59.620	51.600	75.250	60.150
STDM-03	49.710	62.390	47.840	61.650	61.350	17.020	12.610	20.950	45.120	58.420	56.480	50.860	67.480	64.570
STDM-04	52.590	64.770	47.820	58.110	60.720	14.960	14.100	20.160	42.560	76.490	66.870	55.450	74.720	61.430
STDM-05	54.060	64.300	52.940	59.730	60.600	15.500	11.490	20.030	43.590	60.070	55.080	47.130	65.950	60.960
STDM-06	43.780	56.800	50.820	56.000	55.820	13.520	10.420	18.220	38.960	50.590	38.510	53.270	63.610	56.130
STDM-07	46.810	52.470	48.690	54.840	58.330	14.390	10.690	18.490	38.690	51.290	60.950	45.910	61.810	55.250
STDM-08	53.380	59.350	49.670	59.300	61.540	14.090	13.630	19.580	39.950	54.710	53.580	48.480	70.020	59.150
STDM-09	49.940	54.200	46.230	55.630	56.740	15.800	9.250	17.840	39.420	54.020	49.240	44.920	61.510	54.500